Sources and behavior of perchlorate in a shallow Chalk aquifer under military (World War I) and agricultural influences

Feifei Cao, Neil Sturchio, Patrick Ollivier, Nicolas Devau, Linnea Heraty, Jessy J. Jaunat

Sources and behavior of perchlorate in a shallow Chalk aquifer under military (World War I) and agricultural influences

Feifei Cao [(1)], Neil C. Sturchio [(2)], Patrick Ollivier [(3)], Nicolas Devau [(3)], Linnea J. Heraty [(2)], Jessy Jaunat [(1)]

[(1)] *Université de Reims Champagne-Ardenne – GEGENAA – EA 3795, 2 Esplanade Roland Garros, 51100 Reims, France*

[(2)] *Department of Earth Sciences, University of Delaware, 255 Academy Street, Newark, DE 19716, United States*

[(3)] *BRGM, 3 av. C. Guillemin, BP 36009, 45060 Orléans Cedex 2, France*

Corresponding author: Feifei Cao E-mail address: feifei.cao@etudiant.univ-reims.fr

Abstract

Perchlorate (ClO_4^-) has been detected at concentrations of concern for human health on a large scale in groundwater used for drinking water supplies in NE France. Two sources are suspected: a military source related to World War I (WWI) and an agricultural source related to past use of Chilean nitrate fertilizers. The sources and behavior of ClO_4^- have been studied in groundwater and rivers near the Reims city, by monitoring monthly the major ions and ClO_4^- concentrations for two years (2017 – 2019), and by measuring the isotopic composition of ClO_4^- and NO_3^- in water samples. ClO_4^- was detected throughout the study area with high concentrations (> 4 $\mu g \cdot L^{-1}$) detected mainly downgradient of the Champagne Mounts, where large quantities of ammunition were used, stored and destroyed during and after WWI. A WWI military origin of ClO_4^- is inferred from isotopic analysis and groundwater ages. Different tendencies of ClO_4^- variation are observed and interpreted by a combination of ClO_4^- concentrations, aquifer functioning and historical investigations, revealing major sources of ClO_4^- (e.g., unexploded ordnance, ammunition destruction sites) and its transfer mechanisms in the aquifer. Finally, we show that concentrations of ClO_4^- in groundwater seems unlikely to decrease in the short- to medium-term.

Keywords

Perchlorate; Isotope; Groundwater; World War I; Chilean nitrate fertilizer

Highlights

- High ClO_4^- concentrations are detected mainly downgradient of the Champagne mounts.
- ClO_4^- contamination of water comes mostly from WWI military sources.
- Factors governing ClO_4^- transfer in the Champagne Chalk aquifer are evidenced.
- ClO_4^- contamination seems unlikely to decline in the short- to medium-term.

1 Introduction

Perchlorate (ClO_4^-) is an environmental pollutant of growing concern due to its widespread occurrence in water and its adverse health effects by interfering with thyroid uptake of iodine and production of hormones (e.g., Brabant et al., 1992; Braverman et al., 2005; Greer et al., 2002). The high solubility and nonreactivity of ClO_4^- under typical geochemical conditions make it highly mobile in the aquatic environment (Brown and Gu, 2006; Urbansky, 1998). The origin of ClO_4^- in the environment can be synthetic or natural (Cao et al., 2019). ClO_4^- is widely used as an oxidant in solid rocket fuels and explosives (Urbansky, 1998). Therefore, the use and manufacture of these products may constitute an important source of ClO_4^- contamination. Other synthetic sources of ClO_4^- include fireworks, air bags, matches, road flares, chlorate herbicides and bleach products (Aziz et al., 2006; Trumpolt et al., 2005). In natural environments, ClO_4^- can form atmospherically and accumulate by dry and wet deposition in vadose soils in arid and semi-arid environments such as the Atacama Desert (Chile), the southwestern United States, northwestern China, and Antarctica (Jackson et al., 2015, 2016; Lybrand et al., 2016; Rao et al., 2007). The natural NO_3^--rich salt deposits in the Atacama Desert (Chilean nitrate), with ClO_4^- as a minor component (0.1-0.5 wt.%), have been refined and distributed worldwide for use as NO_3^- fertilizer, especially during the first half of the 19th century, thus representing a potential widespread source of ClO_4^- contamination in waters (Ericksen, 1983; Rajagopalan et al., 2006). Over the last two decades, ClO_4^- contamination has been reported from many countries including the USA, Canada, Chile, China, India, UK and France, related to various origins (e.g., Cao et al., 2019, 2018; Furdui et al., 2018; Jackson et al., 2005; Kannan et al., 2009; McLaughlin et al., 2011; Qin et al., 2014; Sturchio et al., 2014; Urbansky, 2002; Vega et al., 2018).

In France, recommended levels of ClO_4^- in drinking water were first issued in 2011 by the French Agency for Food, Environmental and Occupational Health & Safety (ANSES): 15 $\mu g \cdot L^{-1}$ for adults and 4 $\mu g \cdot L^{-1}$ for children under 6 months. The level was subsequently reduced from 15 to 5 $\mu g \cdot L^{-1}$ for adults (ANSES, 2018). According to the national measurement campaign conducted by ANSES from

2011 to 2012, most of the sites having high concentrations of ClO_4^- (> 4 µg·L^{-1}) were located in NE France (ANSES, 2013).

The large extent of ClO_4^- contamination in NE France is unlikely to have been caused by point sources related to industrial activities (Figure 1). However, a potential link between the spatial distribution of high ClO_4^- concentrations and the position of the trench areas of WWI (1914 – 1918) was observed. Thus, a military source of ClO_4^- related to WWI seems likely (Hubé, 2016; Hubé and Bausinger, 2013; Ricour, 2013) but has never been clearly demonstrated. Indeed, synthetic ClO_4^- produced industrially by electrolysis was largely used in explosives manufacturing during WWI. According to Hubé (2014), ~131,000 T of (per)chlorate explosives (primarily composed of NH_4ClO_4 , $KClO_4$, or $NaClO_3$) were used during WWI, mainly in grenade and trench artillery. In addition, ClO_4^- could also be present in other explosives including black powder and nitro group explosives (e.g., TNT, nitroglycerine and nitrocellulose), as Chilean nitrate (with ClO_4^- impurity) was intensively used in the manufacturing of these explosives.

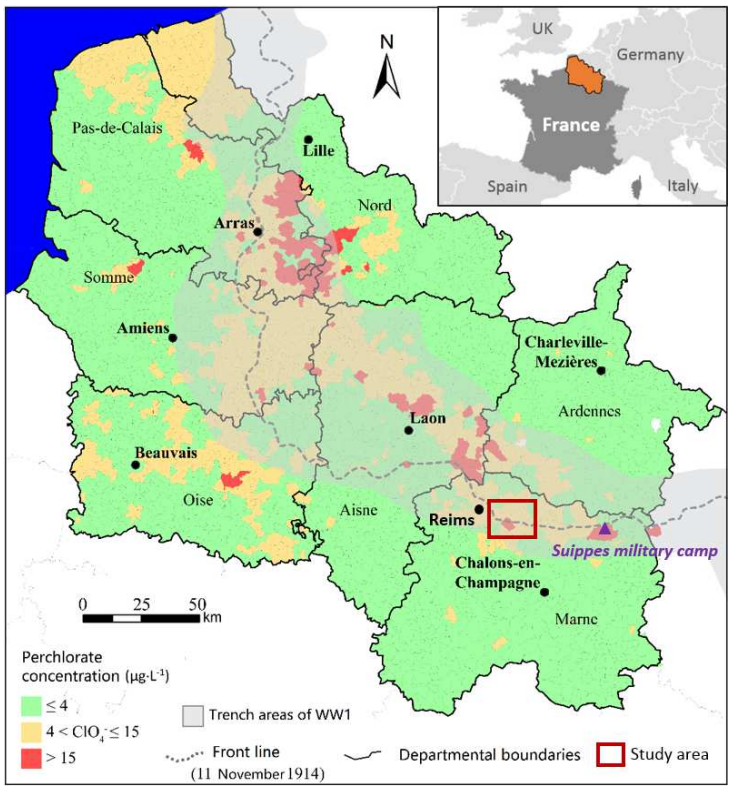

Figure 1 : Distribution of ClO_4^- contamination in groundwater and the positions of the WWI trench areas in NE France (Jaunat et al., 2018)

74 High levels of ClO_4^- have also been detected in some regions outside the trench areas (e.g., Oise, Pas-
75 de-Calais; Figure 1). An agricultural source was suspected, as large quantities of Chilean nitrate was
76 used as fertilizer in France between 1880 and 1950 (Lopez et al., 2015), especially for sugar beet and
77 wheat cultivation (Zimmermann, 1917). Around the year 1928, the estimated amount of Chilean
78 nitrate applied annually for wheat cultivation in France was between 150 and 400 $kg \cdot ha^{-1}$ and could
79 exceed 800 $kg \cdot ha^{-1}$ for beet cultivation (Lopez et al., 2014). For a better management of water
80 resources in NE France, it is now necessary to clarify the source of ClO_4^- contamination (military
81 and/or agricultural). In addition to hydrogeological and historical investigations, isotopic analysis of
82 ClO_4^- can provide a direct approach for ClO_4^- source apportionment.

83 Measurements of stable isotope ratios of chlorine ($^{37}Cl/^{35}Cl$) and oxygen ($^{18}O/^{16}O$, $^{17}O/^{16}O$) and the
84 fractional abundance of the radioactive isotope ^{36}Cl in ClO_4^- ions have shown that three primary
85 source types of ClO_4^- (synthetic; "Atacama" from nitrate salts mined in the Atacama Desert of Chile;
86 and indigenous natural atmospheric deposition) can be clearly distinguished isotopically (Bao and Gu,
87 2004; Böhlke et al., 2017, 2009, 2005; Hatzinger et al., 2011; Jackson et al., 2010; Poghosyan et al.,
88 2014; Sturchio et al., 2014, 2011, 2009, 2006). Additional background information about the ranges of
89 isotopic composition of ClO_4^- is detailed in the references above and summarized in Cao et al. (2019).

90 In this study, a representative study area with two potential sources of ClO_4^- contamination (military
91 and/or agricultural) was selected east of the Reims city in NE France (Figure 1). In this agricultural
92 and military (WWI) context, the primary objectives of this study are to 1) assess the extent of ClO_4^-
93 contamination and its spatio-temporal evolution in the Chalk aquifer, 2) clarify the sources of ClO_4^-
94 contamination (military and/or agricultural) and 3) understand the mechanism of transport and predict
95 the evolution of ClO_4^- in groundwater in the short- to medium- term. To achieve these goals, we used
96 an approach combining continuous monitoring of ClO_4^- concentrations, isotopic composition
97 measurements, historical and hydrogeological investigations, which could be further applied in other
98 ClO_4^- contaminated areas.

2 Materials and methods

2.1 Description of the study area

2.1.1 Location and land use

The study area is situated east of the city of Reims, in the Champagne region in NE France (Figure 1 and Figure 2). It covers about 500 km^2 between the Vesle River (as the southern boundary) and the Suippe River (as the northern and eastern boundaries; Figure 2). Land use in this area is largely agricultural (> 80%) with wheat, barley, sugar beet, and alfalfa as major crops. Forest covers about 15% of the study area, mainly on the Berru and Champagne Mounts and the riparian areas. Urban lands including towns, villages, and industrial sites represent only about 3% of the study area (CORINE Land Cover geographic database).

2.1.2 Geological and hydrogeological context

A detailed geological and hydrogeological description of the study area is given by Cao et al. (2020). The Chalk formation (Upper Cretaceous, 66 – 100 Ma) constitutes almost the entire surface of the study area, with only a limited exposure of Tertiary formation at Berru Mount (Figure 2). The Tertiary formation includes a succession of permeable (sand and coarse limestone) and impermeable deposits (clay and marl) where only a few thin aquifers of limited extent are developed with some springs flowing from the sand layers (Laurain et al., 1981). These aquifers are insufficiently productive to be used as drinking water supplies. The Chalk formation of the study area includes Coniacian (C3), Santonian (C4) and Campanian (C5) Chalks (Figure 2), which have similar lithology and hydrodynamic properties despite their different ages of formation. It is a pure, fine-grained carbonate rock, characterized by dual porosity (matrix and fracture) providing both slow and rapid flowpaths for groundwater (e.g., Foster, 1975; Headworth et al., 1982; Price, 1987). The total porosity of the Chalk is about 40% (Crampon et al., 1993) with only 1% effective porosity (Vachier et al., 1987). The first 10-20 m of the Chalk is significantly fractured; the density of fractures decreases with depth and distance to river valleys (Allen et al., 1997; Mangeret et al., 2012; Vachier et al., 1987). In addition,

the Chalk formation is partially covered by superficial (Quaternary) formations including graveluche (a periglacial formation up to 10 m thick), colluvium (1-3 m thick) and alluvium (up to 10 m thick) with relatively high content of clay and silt (Allouc et al., 2000; Vernhet, 2007) (Figure 2).

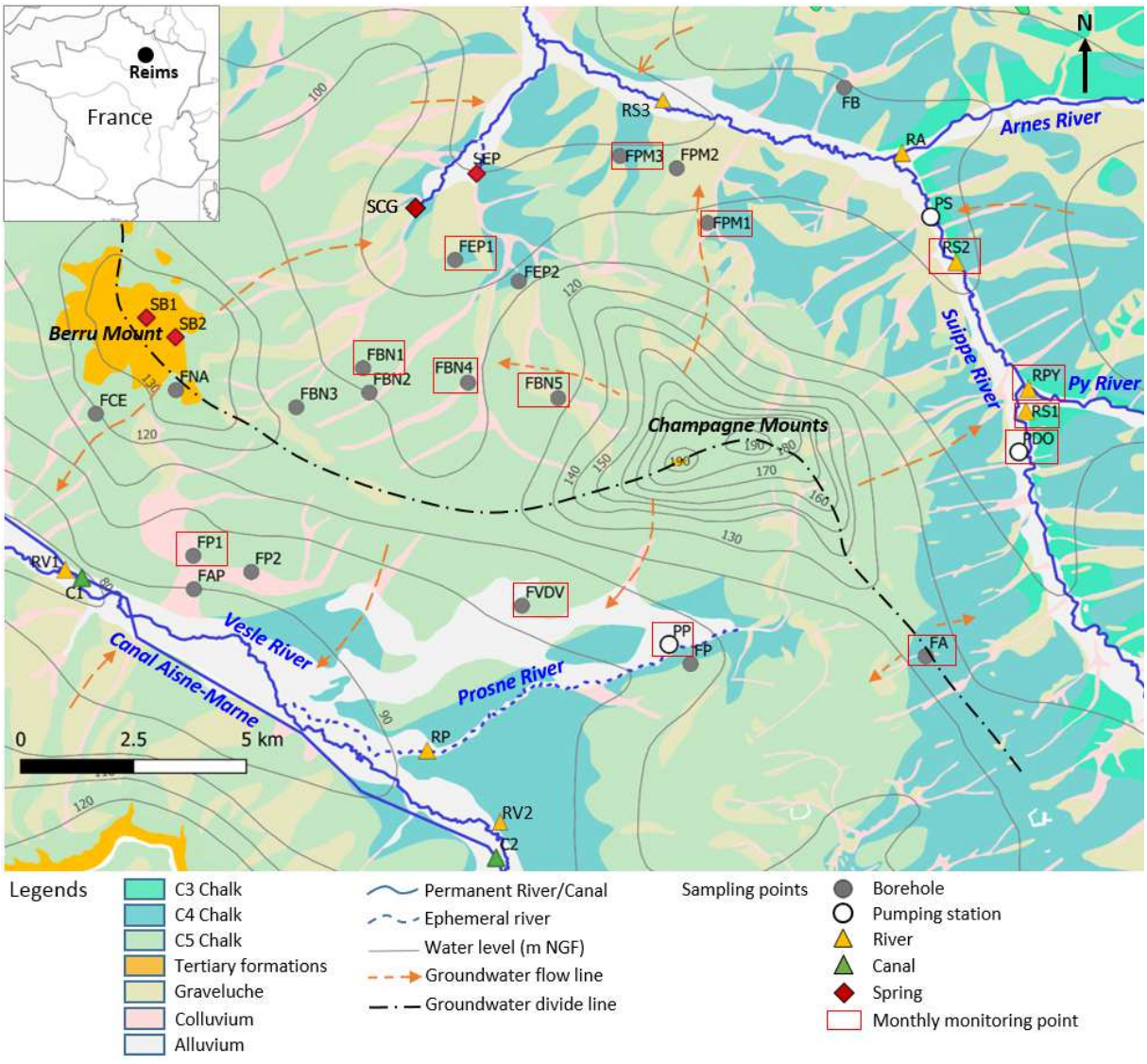

Figure 2 : Geological and hydrogeological map of the study area recorded at high water level with the location of sampling points (modified from Cao et al., 2020). Source of geological map: Laurain et al. (1981), Allouc and Le Roux. (1995); source of water level data: Rouxel-David et al. (2002a).

The chalk aquifer is an important groundwater resource of the region. Precipitation is the only recharge source of the aquifer, mainly from November to March, due to the excess of rainfall compared to evapotranspiration (Cao et al., 2020; Chiesi, 1993). The surface runoff is usually considered as very low or absent for the Champagne Chalk aquifer (Chiesi, 1993; Foster, 1975;

Mathias et al., 2006). The study area is divided into two parts by the groundwater divide line across the summit of Berru Mount and the Champagne Mounts, which delimits the Vesle River watershed in the south and the Suippe River watershed in the north (Figure 2).

2.1.3 Suspected sources of ClO_4^- contamination

Groundwater contamination by ClO_4^- in the study area is potentially caused by both the WWI-related military source and the agricultural source related to the past use of Chilean nitrate fertilizer. The study area was intensively marked by events of WWI (Facon, 2018; Laurent, 1988). As shown in Figure 3, almost the entire study area was crossed by trenches, particularly in the center of the area (Taborelli, 2018). From 1914 to 1918, these trench areas were the scenes of several intensive battles of WWI (e.g., the Battles of Champagne), especially on the Champagne Mounts. During WWI, military tunnels were dug by the German army, such as the tunnels of Mont Cornillet (N1), Mont Perthois (N2) and Mont sans Nom (N3) (Figure 3). These tunnels, usually equipped with quantities of ammunition, connected the German front positions with the rear and allowed the German army to fire until the last moment. It is highly probable that quantities of ammunition still remain underground at these sites, representing potential sources of groundwater contamination of ClO_4^- and other pyrotechnic compounds. Furthermore, it is likely that the precise locations of some of these underground sites are unknown.

After WWI, large quantities of unused ammunition were still present on the French land and it was necessary to clear the battlefield in order to make these lands habitable and cultivable on a large scale. Thus, unused ammunitions were either dismantled to recycle valuable materials or destroyed by explosion. The ammunition explosion sites were recognizable in historical aerial photographs by anthropogenic forms such as alignments of shell-holes, an access road, and a storage area. Several explosion sites were identified in the study area from inspection of historical aerial photographs (IGN Remonter le temps database; Figure 3). While traces of N5 and N6 could no longer be recognized, the destruction activities on site N1 lasted until the 2000s and some military wastes are still present at this site (BASOL database). The sites and activities listed are not exhaustive since the compilation is based

on existing data from historical archives and/or former aerial photographs that did not cover the entire study area. In addition, traces of military activities could have been quickly erased, making it difficult to identify all related sites. The ammunitions exploded on battlefields during WWI or destroyed after the war could have released ClO_4^- into the environment. In addition, large quantities of unexploded ammunitions (about 30% of the total quantity of ammunition used) could still persist in the subsoil (Desailloud and Wemeau, 2016), representing a continuous and diffuse source of ClO_4^-contamination.

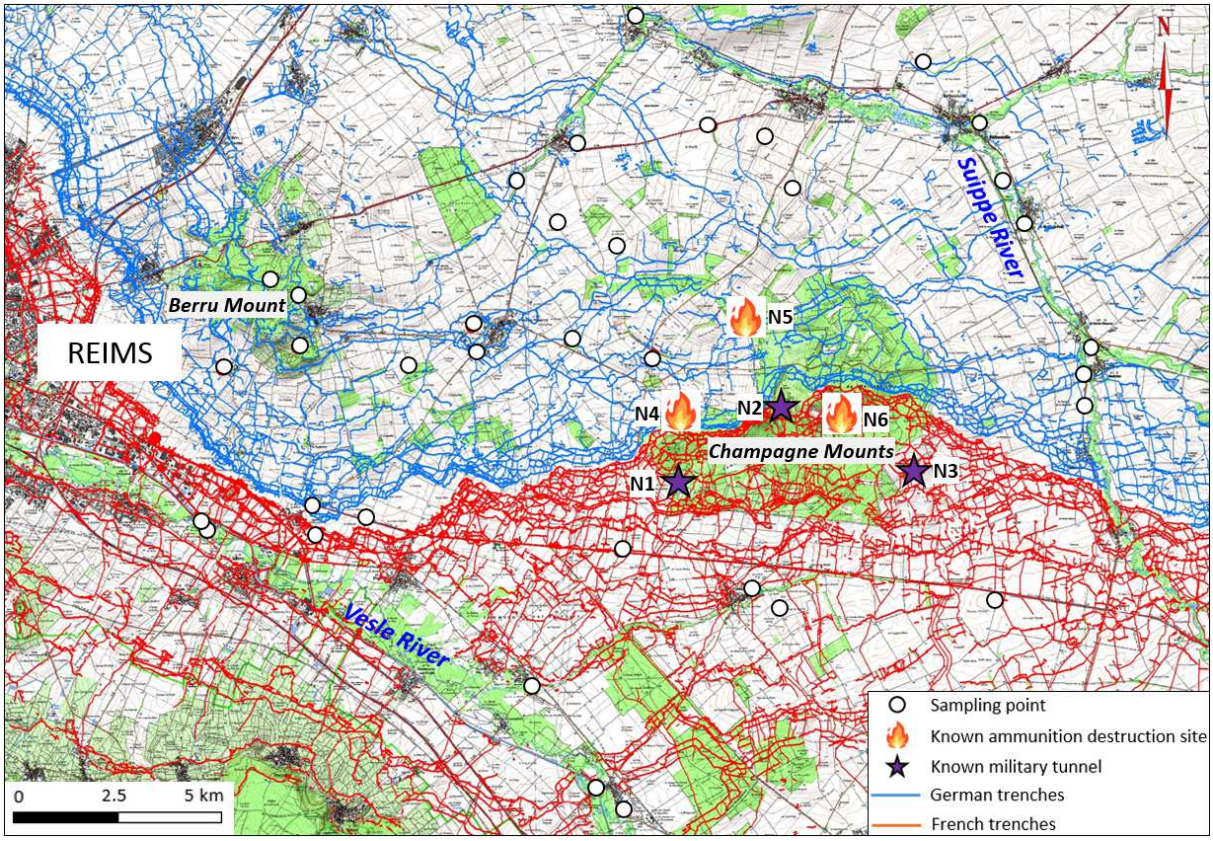

Figure 3 : Trenches, military tunnels and ammunition destruction sites related to WWI on the study area (position of trenches from Taborelli, 2018)

As a traditional agricultural area for wheat and sugar beet, the study area was extensively cultivated with the use of Chilean nitrate fertilizer from 1880 to 1950. It was estimated that the average annual consumption of nitrogen in Marne (the department where the study area is located) was between 7,000 and 10,000 T in the 1950s (Lopez et al., 2014). The use by spreading and the storage of these Chilean nitrates could represent diffuse or point sources of ClO_4^- contamination in groundwater.

2.2 Sampling and analysis methods

An intensive sampling network was established in the study area with a total of 36 sampling points including 26 groundwater (19 boreholes, 3 pumping stations and 4 springs) and 10 surface water (2 in the Aisne-Marne Canal, 2 in the Vesle River, 3 in the Suippe River and 3 in their tributaries) (Figure 2), as surface water is here closely related to groundwater of the Chalk aquifer. The boreholes and pumping stations have long screen depths which cover at least half of the well depths (Table 1), thus providing a weighted average of groundwater. A first screening campaign was carried out in June 2017, which yielded a chemical map of the study area and the extent of ClO_4^- contamination. Fourteen sampling points (primarily points with high concentrations of ClO_4^-, well distributed in the study area; Figure 2) were then selected for monthly monitoring for 2 years to observe the spatio-temporal evolution of groundwater geochemistry and ClO_4^- concentrations. In addition, groundwater ages, water flow rate in rivers, explosive concentrations, and isotopic compositions of ClO_4^- and NO_3^- were measured.

The measurement methods and results of groundwater level, physico-chemical parameters, major ions and groundwater dating using CFCs and SF_6 have been fully described and interpreted previously in Cao et al. (2020). These results are directly used in this study.

Water discharge of rivers was measured by the cross-section method using an OTT C2 Small Current Meter. ClO_4^- was analyzed by ion chromatography at BRGM (Orléans, France) with a quantification limit of 0.5 $\mu g \cdot L^{-1}$. Thirty-nine explosives (see SI.1) were analyzed in waters with an RPHPLC-DAD system by the company Envilytix GmbH (Wiesbaden, Germany), as described by Bausinger et al. (2007).

Isotopic analyses of ClO_4^- were carried out in water samples collected from 3 sites in the study area: FBN4 (at high and low water levels), FVDV (at high water level) and PY (at high water level; Figure 2). In order to obtain a pure military isotopic signature of ClO_4^-, a water sample was also collected at the limit of the Suippes Military camp (outside the study area; Figure 1), as the only source of ClO_4^- here that is related to WWI without any potential agricultural influence. Water samples were collected

using PVC columns containing ClO_4^- specific ion exchange resin (IX resin) and then purified and analyzed as described previously by Gu et al. (2011), Hatzinger et al. (2011, 2018), and Böhlke et al. (2017). The extraction and purification of ClO_4^- was done in the Department of Civil and Environmental Engineering of Texas Tech University (USA) and the key steps can be summarized as follows: 1) the resin was washed by deionized water and flushed with 4M HCl to remove NO_3^-, SO_4^{2-}, HCO_3^- and organics; 2) the absorbed ClO_4^- was eluted from the IX resin using a solution of 1M $FeCl_3$ and 4M HCl (Gu et al., 2007, 2001; Gu and Brown, 2006); 3) eluted ClO_4^- was purified by a series of precipitation, liquid-liquid extraction, evaporation, and cation exchange processes, then crystallized as a ClO_4^- salt for isotopic analysis. The relative abundances of stable isotopes of chlorine (^{37}Cl and ^{35}Cl) and oxygen (^{18}O, ^{17}O and ^{16}O) in ClO_4^- were measured using isotope-ratio mass spectrometry (IRMS) at the Environmental Isotope Geochemistry Laboratory of the University of Delaware (USA).

For isotopic analysis of NO_3^-, water samples were collected in 100-mL polyethylene bottles after filtration through 0.45 µm membranes. Nitrogen and oxygen isotope ratios were measured using an automated denitrifier method as described in Morin et al. (2009) and Savarino et al. (2013). This technique uses *Pseudomonas aureofaciens* bacteria to convert NO_3^- to N_2O, which is then analyzed for its isotopic composition after thermal decomposition to O_2 and N_2. Isotopic analysis was performed on a Thermo Finnigan MAT253 equipped with a gas-bench interface at the Laboratoire de Glaciologie et Géophysique de l'Environnement at the University of Joseph Fourier Grenoble (France).

2.3 Statistical analysis methods

Interactions between ClO_4^- concentrations and groundwater level as well as major ions were calculated by using an approach based on a semi-parametric regression model. More precisely, a generalized additive model (GAM) with cubic splines accounting for autocorrelation of data through a first order autoregressive model (AR1) was used. Each GAM was carried out using the Akaike information criterion (AIC) score and the likelihood ratio. The corresponding adjustment coefficient of determination (Adj. R^2) associated with a significance test at a P-value < 0.05 was used to characterize correlations between response variable and the explicative one.

227 The GAM was also adopted to decipher time-dependent changes in perchlorate concentrations. A
228 model was built for each of the 14 sampling points, which were monitored monthly. Each of these
229 GAM was built considering a Gamma distribution of perchlorate concentration and the log link
230 function was used as it was the most appropriate for this kind of distribution. Two time-dependent
231 smooth functions were used to build each model. Seasonal changes in perchlorate concentrations are
232 represented by the first term taking into account days of year. The penalized cubic regression spline
233 was used for this smooth function to allow a nonlinear response of perchlorate to time during a
234 calendar year. The second term was constructed to filter out the long-term trends (inter-annual
235 variations). For convenient output, we have redefined the time-scale for this term as a continuous
236 variable. For this second term, the thin plate regression spline was used.

237 For the two smooth functions, the smoothness was controlled by the number of knots and the
238 associated effective number of degrees of freedom. The optimal number of knots was estimated
239 through cross-validation. In consequence, the basis dimension for the two smooth functions was
240 adapted to have enough degrees of freedom to fit the data while these values remained small enough to
241 maintain reasonable computational efficiency and avoided over-fitting the data. For the two smooth
242 functions, the method of the finite difference was used to calculate the first derivative of the function
243 and the associated confidence interval. This first derivative was used to estimate the rate of change to
244 identify periods of statistically significant change (either increase or decrease in perchlorate
245 concentration).

246 The underlying assumption of homogeneity for model residuals has been checked by plotting deviance
247 residuals against fitted values. QQ plots (sample quantiles against theoretical quantiles) and Shapiro
248 tests were used to assess normality of the model residuals. We have examined autocorrelation of the
249 model residuals; the autocorrelation function values showed that the model residuals were not
250 correlated as they dropped to small values within a couple of days. Validity of the model was also
251 assessed through AIC score and Adj.R^2. Analysis of deviance was used to assess the significance of

252 the null hypothesis for the two smooth functions. All statistical tests were carried out using R-software
253 (R core Team, 2018).

3 Results and discussion

3.1 Occurrence of ClO_4^- and explosives

Perchlorate was detected at almost all sampling sites (33 out of 36) (Table 1). Mean ClO_4^- concentrations measured during the two years monitoring were > 4 $\mu g \cdot L^{-1}$ at 17 sites, including two sites with mean concentrations > 15 $\mu g \cdot L^{-1}$, representing 49% and 6% of the sampling sites, respectively. Low concentrations (< 4 $\mu g \cdot L^{-1}$) were measured at 19 sites, representing 51% of the sampling points.

Table 1 : Properties of sampling points, water table depth, concentrations of Cl^-, NO_3^- and ClO_4^- and isotopic compositions of NO_3^- in ground- and surface water samples (N: number of sampling; NA: not available. -: not applicable)

Name	Type	N	Depth (m)	Screen depth (m)	Water table depth (m)	Cl^- ($mg \cdot L^{-1}$)	NO_3^- ($mg \cdot L^{-1}$)	ClO_4^- ($\mu g \cdot L^{-1}$)	NO_3^- $\delta^{18}O$ (‰)	NO_3^- $\delta^{15}N$ (‰)
FA	Borehole	21	35	3.5 - 30	2 - 6	35.4 ± 6.3	39.7 ± 6.0	3.1 ± 0.9	-1.4	-0.7
FAP	Borehole	21	15	6.5 - 15	3 - 12	30.7 ± 9.5	28.4 ± 6.7	5.4 ± 2.2	-1.9	1.7
FBN1	Borehole	21	48	4 - 48	26 - 40.5	25 ± 8.8	28.9 ± 7.6	3.6 ± 1.7	2.1	3.9
FBN4	Borehole	21	28	16 - 28	2.5 - 18	52.9 ± 2.6	54.3 ± 2.6	20.8 ± 3.2	-0.6	1.0
FBN5	Borehole	21	47	24 - 43	22.5 - 35	15 ± 9.2	31.6 ± 11.3	7.9 ± 3.7	-0.6	1.1
FEP1	Borehole	21	25	7 - 25	7.5 - 17	35.2 ± 1.0	36.7 ± 1.4	12.9 ± 2.4	-0.3	0.5
FP1	Borehole	21	19	9 - 15	4.5 - 13	28 ± 2.9	29.9 ± 3.9	6.6 ± 1.9	-1.3	1.1
FPM1	Borehole	21	24	NA	NA	7.6 ± 0.7	19 ± 0.8	14.1 ± 2.0	-1.4	0.4
FPM3	Borehole	21	21	7 – 21	9 - 18	18.6 ± 5.0	24 ± 5.7	3.5 ± 0.8	-0.5	0.3
FVDV	Borehole	21	22	12.5 - 21	7 - 15	39 ± 1.6	40 ± 2.3	44.4 ± 6.9	-1.7	0.8
PDO	Pumping station	21	25	7 - 25	NA	33.9 ± 1.2	42.1 ± 2.0	11.5 ± 1.7	-1.8	0.6
PP	Pumping station	21	80	23 - 80	NA	21.8 ± 1.1	25.8 ± 0.9	9.2 ± 4.0	-1.5	0.0
PS	Pumping station	4	16	7 - 16	NA	23.6 ± 1.4	32.4 ± 2.7	4.1 ± 1.4	-0.2	1.6
FCE	Borehole	1	85	NA	NA	7.2	3.1	0.5	NA	NA
FNA	Borehole	1	47	NA	NA	20.0	24.3	1.3	NA	NA
FBN3	Borehole	3	56	12 - 56	16 - 22	13.4 ± 2.4	15.2 ± 2.2	1.3 ± 0.4	5.4	7.5
FBN2	Borehole	4	32	10 – 32	17 - 26	31.6 ± 4.1	18.2 ± 12.5	2 ± 1.7	6.6	10.3
FEP2	Borehole	6	23	NA	15 - 18.5	8.8 ± 0.6	9.5 ± 0.8	2 ± 1.3	-0.3	-0.5
FPM2	Borehole	5	35	NA	30 - 31	16.2 ± 5.1	22.1 ± 5.2	6.1 ± 0.6	-1.3	0.6
FP2	Borehole	4	21	NA	8 - 13	165.8 ± 18.9	38 ± 3.3	1.2 ± 0.7	-0.9	3.6
FP	Borehole	4	23	7 – 22.5	12 - 17	39.0 ± 3.3	45 ± 5.0	5.9 ± 0.9	-1.7	0.6
FB	Borehole	1	33	NA	12.8	28,0	36.6	2.2	NA	NA
SEP	Spring	12	-	-	-	23.5 ± 1.9	33.1 ± 2.6	5.5 ± 3.0	-1.5	1.8
SCG	Spring	2	-	-	-	28.5 ± 0.2	40.7 ± 0.1	4.7 ± 2.1	NA	NA
SB1	Spring	1	-	-	-	16.5	7.8	< 0.5	NA	NA
SB2	Spring	1	-	-	-	18.4	2.3	2.1	NA	NA
RS1	Suippe River	21	-	-	-	25.8 ± 1.2	29.3 ± 1.9	3.4 ± 0.8	1.0	3.7
RPY	Py River	21	-	-	-	20.7 ± 1.5	28.5 ± 1.6	11.6 ± 3.1	NA	NA
RS2	Suippe River	21	-	-	-	24.3 ± 1.3	29.6 ± 1.3	6.5 ± 2.1	0.8	2.6
RA	Arnes River	4	-	-	-	22.1 ± 1.0	26.1 ± 1.2	1.5 ± 1.0	0.4	3.1
RS3	Suippe River	4	-	-	-	25.2 ± 0.4	28.8 ± 0.8	5.1 ± 1.5	0.4	3.1
RV1	Vesle River	3	-	-	-	29.3 ± 1.1	25.9 ± 3.7	1.2 ± 0.5	0.7	5.9
RV2	Vesle River	3	-	-	-	25 ± 1.9	28.5 ± 2.8	0.9 ± 0.4	0.4	4.7
RP	Prosnes River	1	-	-	-	21.3	25.6	3.6	NA	NA
C1	Canal	1	-	-	-	18.3	12.7	< 0.5	NA	NA
C2	Canal	1	-	-	-	15.5	13.1	< 0.5	NA	NA

263 An analysis of the geographic distribution of ClO_4^- is presented in Figure 4, revealing some major
264 trends and potential sources of ClO_4^-. Lower concentrations of ClO_4^- (< 4 $\mu g \cdot L^{-1}$) were mainly found
265 on the Berru Mount, in the Vesle River and in the Aisne-Marne Canal. As mentioned above, the
266 Tertiary formation on the Berru Mount is represented by a succession of permeable and impermeable
267 layers, which contains several small aquifers in which water could be renewed quickly by precipitation.
268 As a result, low levels of ClO_4^- were detected in this area. In the Vesle River, ClO_4^- concentrations
269 ranged from 0.9 ± 0.4 $\mu g \cdot L^{-1}$ to 1.2 ± 0.5 $\mu g \cdot L^{-1}$. The Vesle River originates far away upstream,
270 receiving groundwater discharge from outside the study area that is little affected by ClO_4^-
271 contamination. In the Aisne-Marne Canal, ClO_4^- was not detected (< 0.5 $\mu g \cdot L^{-1}$), indicating that the
272 canal has little or no input from the contaminated groundwater or river water (Vesle River) of the
273 study area.

274 Most of the sampling sites with ClO_4^- concentrations exceeding 4 $\mu g \cdot L^{-1}$ were located downgradient of
275 the Champagne Mounts (Figure 4), where large quantities of ammunitions were used, stored, and
276 destroyed during and after WWI. The highest concentrations of ClO_4^- were found at borehole FVDV,
277 with a maximum of 62.5 $\mu g \cdot L^{-1}$ (in September 2018) and an average of 44.4 ± 4.9 $\mu g \cdot L^{-1}$. Plume-like
278 patterns of ClO_4^- were observed along the sections A – A' and B – B' (the same direction as the
279 groundwater flow line; Figure 4). At FBN4, FEP1 and SEP (A – A'), mean ClO_4^- concentrations over
280 the two years monitoring were 20.8 ± 3.2 $\mu g \cdot L^{-1}$, 12.9 ± 2.4 $\mu g \cdot L^{-1}$ and 5.5 ± 3.0 $\mu g \cdot L^{-1}$ respectively,
281 indicating a progressive decrease with distance downgradient. A similar pattern was observed at FPM1,
282 FPM2 and FPM3 (B – B') with concentrations of 14.1 ± 2.0 $\mu g \cdot L^{-1}$, 6.1 ± 0.6 $\mu g \cdot L^{-1}$ and 3.5 ± 0.8
283 $\mu g \cdot L^{-1}$ respectively. The high ClO_4^- levels and the observed plume-like patterns indicated that potential
284 point-sources of ClO_4^- could be present upstream at FVDV, FBN4 and FPM1. Specifically, the
285 military tunnel N1 and the ammunition destruction sites (N4 and N5) were likely responsible for the
286 high concentrations of ClO_4^- measured at these sites (Figure 4).

287 Although ClO_4^- concentrations in river waters were generally lower than those of groundwater, some
288 river sites had relatively high ClO_4^- concentrations (>10 $\mu g \cdot L^{-1}$), such as RPY in the Py River (Figure 4

and Table 1). The Py River is downstream from the Suippes military camp that represents a potential source of ClO_4^- contamination to the Py river watershed (Figure 1). In the Suippe River upstream of the confluence with the Py River (RS1), low ClO_4^- concentrations (3.4 ± 0.5 µg·L^{-1}) were measured while, downstream of this confluence (RS2), higher concentrations (6.5 ± 2.1 µg·L^{-1}) were found.

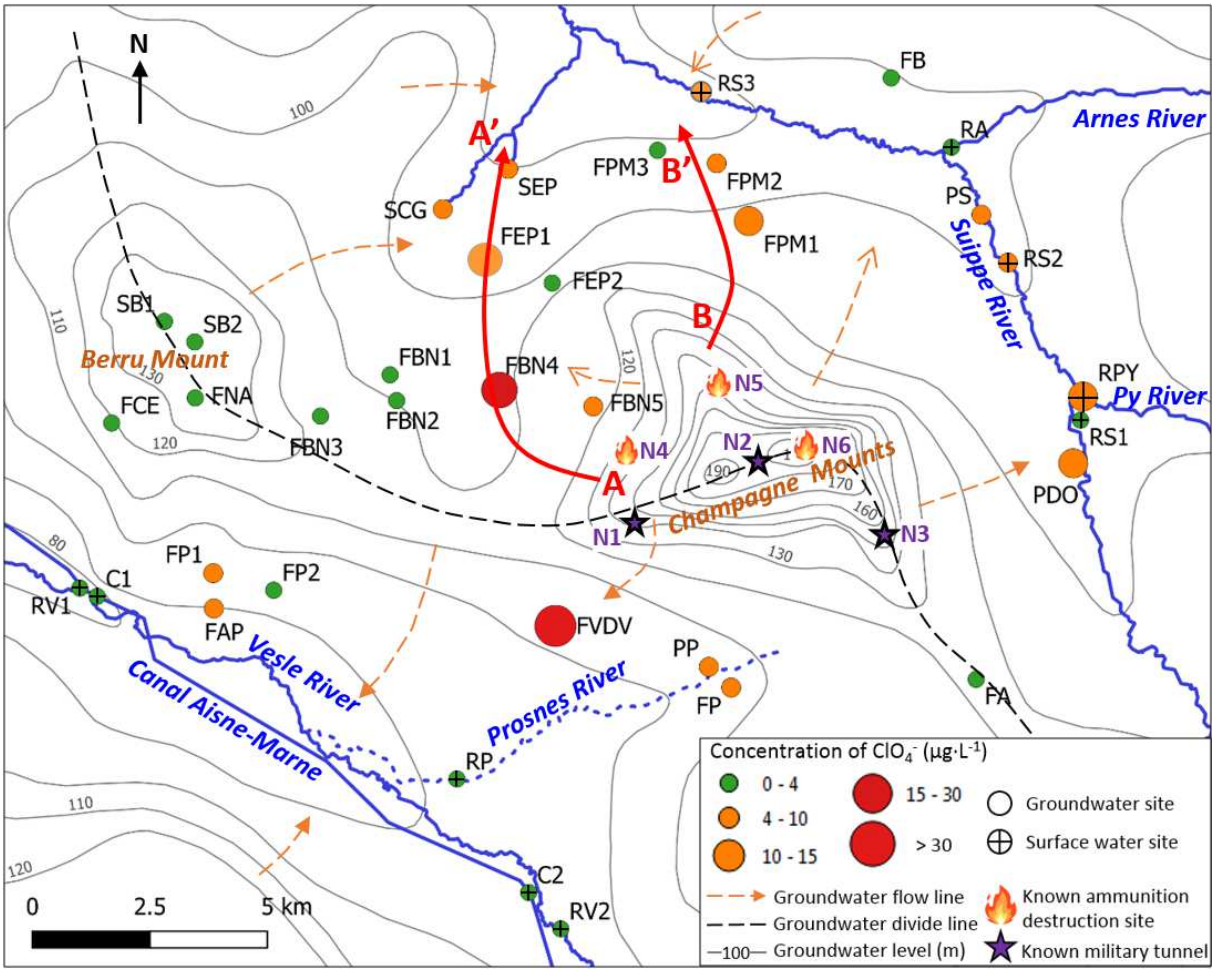

Figure 4 : Spatial distribution of ClO_4^- contamination on the study area and military sites related to the WWI

Unlike the widespread contamination of ClO_4^- on the study area, organic explosives have not been detected in surface and groundwater samples, which could be explained by their low persistence and mobility in soil and water (Clausen et al., 2006). During WWI, nitro group explosives such as TNT, nitroglycerine and nitrocellulose were largely used. TNT can be rapidly degraded in most soil and aquifer systems; therefore, its presence is typically restricted to areas near its introduction to the environment. At most sites, TNT can be completely attenuated in the surface soil, thereby preventing

contamination of the unsaturated zone (UZ) or groundwater (Clausen et al., 2006). Nitroglycerin is soluble when present alone and is subject to rapid biodegradation, but when present with nitrocellulose it is insoluble. Nitrocellulose is also insoluble, resulting in its low mobility in the environment (Quinn, 2015).

3.2 Sources and fate of ClO_4^- in the Chalk aquifer

3.2.1 Isotopic composition of ClO_4^- and NO_3^-

The results of Cl and O stable isotope analysis for ClO_4^- in water samples are presented by dual isotope plots in comparison to published data for synthetic, Atacama and selected US indigenous natural ClO_4^- occurrences (Table 3 and Figure 5). There is no evidence of ClO_4^- biodegradation, which is consistent with the typical oxic condition of the unconfined Chalk aquifer (Barhoum et al., 2014; Edmunds et al., 1987); the isotopic composition of ClO_4^- could therefore reflect initial values of the sources.

Table 3 : Isotopic compositions of ClO_4^- in ground- and surface water samples (HW: high water; LW: low water)

Name	Sample date	$\delta^{18}O$ (‰)	$\Delta^{17}O$ (‰)	$\delta^{37}Cl$ (‰)
FVDV	04/05/18	-20,7	0,2	0,3
FBN4 (HW)	04/06/18	-21,8	0,2	0,2
FBN4 (LW)	01/18/19	-29,6	-0,3	-3,3
RPY	04/10/19	-22,9	1,3	-6.0
RM	02/22/19	-18,2	0,1	-0,2

The $\delta^{37}Cl$, $\delta^{18}O$ and $\Delta^{17}O$ values of ClO_4^- in water samples collected at the Suippe military camp (RM; pure military source), FVDV and FBN4 (at high water level) plotted exactly within the synthetic ClO_4^- range, proving similar military sources of ClO_4^- at these sites (Figure 5). However, the results for FBN4 (at low water level) was different, with a lower $\delta^{18}O$ value (-29.6‰) falling outside the published synthetic ClO_4^- ranges. Nevertheless, the $\delta^{37}Cl$ and $\Delta^{17}O$ values (-3.3‰ and -0.3‰, respectively) were typical of synthetic ClO_4^-. Therefore, ClO_4^- at FBN4 (at low water level) was interpreted as of synthetic origin, but different from other samples and currently reported synthetic ClO_4^- products. Indeed, the manufacturing processes of synthetic ClO_4^- and the materials used more than 100 years ago during WWI may be different from those of today. Even during WWI, different ClO_4^- salts (NH_4ClO_4 and/or $KClO_4$) were used in explosives; they were produced in different facilities

and the method could also have evolved during the WWI conflict. This could possibly explain why this "unusual" synthetic end-member was observed at FBN4 (at low water level). The different ClO_4^- isotopic compositions observed at FBN4 at high and low water levels suggest that there could be different sources of ClO_4^- at different depths. The estimated groundwater ages in the study area were less than 50 years (Cao et al., 2020). Moreover, because the thickness of UZ is less than 30 m (Table 1) and considering that the flow rate is about 1 $m \cdot year^{-1}$ through the Chalk matrix, the time of transfer in the UZ were less than 30 years (e.g., Barraclough et al., 1994; Brouyère et al., 2004; Chen et al., 2019; Wellings, 1984). Therefore, military sources of ClO_4^- contamination are most likely related to military activities after WWI (destruction of ammunitions) rather than during the conflict, or to the release of ClO_4^- from unexploded ordnance persisting in the subsoil (or unused ammunitions stored on the surface).

In the RPY sample, a substantial fraction of ClO_4^- with an Atacama-type isotopic composition is evident. The lower value of $\delta^{37}Cl$ (-6.0‰) and the higher value of $\Delta^{17}O$ (+1.3‰) are both consistent with a mixture of a synthetic end-member with typical Atacama ClO_4^-. This could probably be explained by the nitrogen explosives of WWI (black powder and nitro group explosives) made with Chilean nitrate and/or the past use of Chilean nitrate as fertilizer. Indeed, the PY River water consists of aquifer discharge from the entire watershed. Although synthetic (military) ClO_4^- is indicated by isotopic analysis at two sites with the highest ClO_4^- concentrations (FVDV and FBN4), Atacama ClO_4^- from Chilean nitrate fertilizer might be present, especially at sites with low ClO_4^- concentrations related to diffuse sources.

The NO_3^- isotope data at all the sampling points did not show any evidence of an Atacama source for the NO_3^- (Figure 5). However, this cannot rule out the possibility of the existence of Atacama NO_3^- in water samples, as Atacama NO_3^- could have been replaced and/or assimilated with the biogenic NO_3^- in the soil (Böhlke et al., 2009). Indeed, the distinctive isotopic composition of oxygen in atmospheric NO_3^- is preserved only in hyper-arid environments and is lost in moist soils where higher biological activity occurs (Böhlke et al., 1997; Michalski et al., 2015). Therefore, more information is needed to

better evaluate the regional extent of ClO_4^- sources related to the past use of Chilean nitrate in the study area.

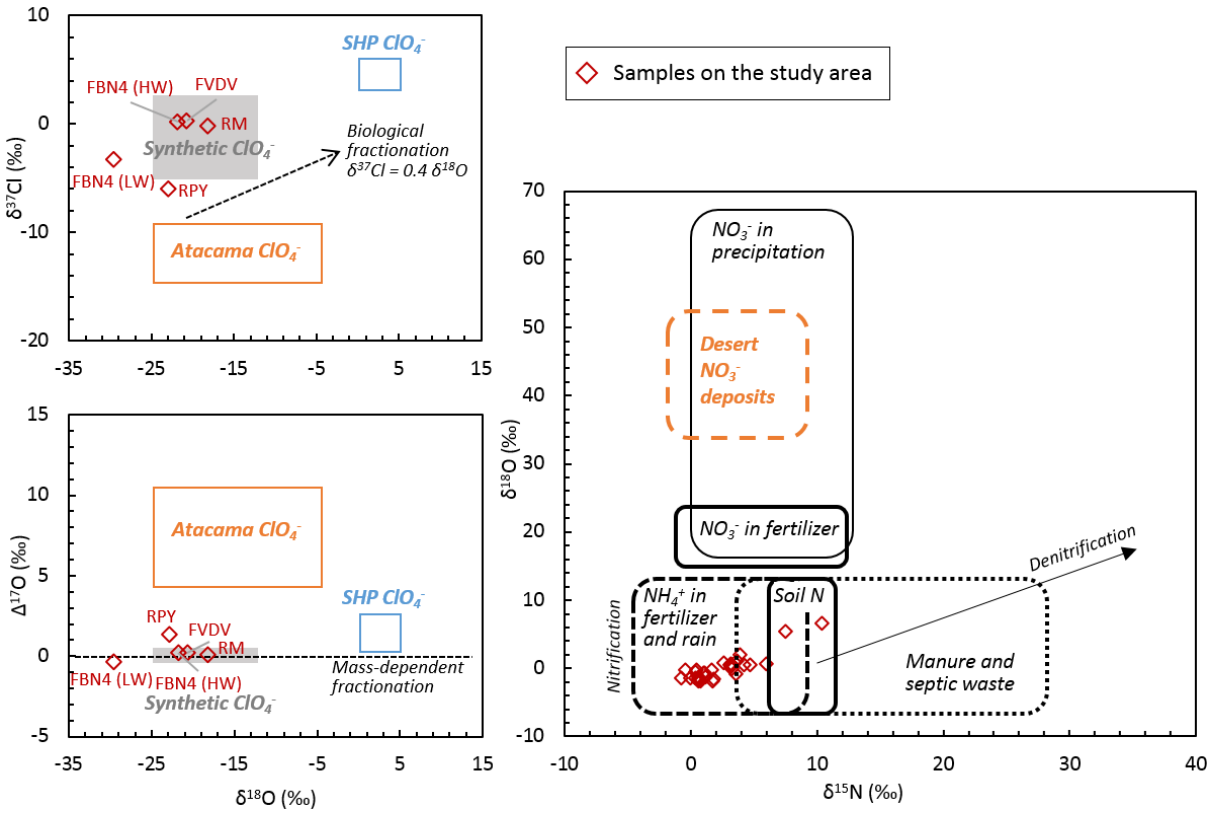

Figure 5: Summary of isotope data for ClO_4^- and NO_3^- in water samples of the study area, compared with major known ClO_4^- sources including synthetic, Atacama and indigenous natural ClO_4^- from the Southern High Plains (Texas) (SHP) (Ader et al., 2001 ; Bao and Gu, 2004 ; Böhlke et al., 2005, 2009 ; Jackson et al., 2005b, 2010 ; Parker et al., 2008 ; Plummer et al., 2006 ; Rajagopalan et al., 2006 ; Rao et al., 2007 ; Sturchio et al., 2007, 2011). Arrow in the $\delta^{37}Cl$ vs $\delta^{18}O$ graph represents the slope of biodegradation ($\delta^{37}Cl$ = 0.4 $\delta^{18}O$) and arrow in the $\Delta^{17}O$ vs $\delta^{18}O$ graph represents the direction of mass dependent fractionation.

3.2.2 Temporal variability of ClO_4^- compared with groundwater levels and major ions

The temporal variation of ClO_4^- concentrations measured from June 2017 to June 2019 was compared with groundwater level fluctuation and the temporal variation of NO_3^- and Cl^- concentrations (two major agriculture-derived ions, Cao et al., 2020), in order to explore the potential sources of ClO_4^- (point and/or diffuse source), and the possible future evolution of ClO_4^- in the Chalk aquifer.

At most sites, inter-annual variations of ClO_4^- concentrations were observed and also revealed by the statistical trend analysis (Figure 6 and Table 4). The periods when ClO_4^- concentrations changed significantly under the seasonal and annual effects were estimated with the statistical methods

367 presented in section 2.3 (results detailed in SI.2). Higher ClO_4^- concentrations were observed in 2018
368 (Figure 6 and SI.2), corresponding with the higher groundwater level in 2018.

369 *Table 4 : Seasonal and annual effects on ClO_4^- concentrations (the effect is considered as statistically significant with P-*
370 *value < 0.05, related values < 0.05 are marked in bold)*

	Seasonal trend	Annual trend
FVDV	0,079	**> 0.001**
FBN4	0,097	0,209
FEP1	0,052	0,291
FBN5	**0,003**	**0,007**
FA	0,176	**0,015**
FBN1	0.028	0,374
FP1	0,161	0,165
FPM3	0,067	**0,033**
RS1	0,053	0,767
RPY	**0,021**	**0,022**
RS2	**0,011**	0,240
PDO	0,624	0,135
FPM1	0,097	**> 0.001**
PP	**0,012**	0,326

371 At sites having mean ClO_4^- concenrations > 10 µg·L^{-1} (FVDV, FBN4, FEP1 and FBN5; Figure 6),
372 several peaks of ClO_4^- concentration were observed and the temporal variation of ClO_4^- was poorly
373 correlated with the groundwater level fluctuation (Table 5). The peaks could possibly be explained by
374 localized flushing of ClO_4^- from the UZ by natural (rainfall) or artificial (irrigation) recharge processes,
375 indicating the presence of point sources of ClO_4^- contamination upstream of these sites. At FVDV and
376 FBN4, the two most contaminated sites, the correlation coefficients between ClO_4^- and groundwater
377 level were the lowest (Table 4 and Figure 6), as ClO_4^- concentrations here were mainly controlled by
378 the ClO_4^- transfer waves following flushing rather than the groundwater level fluctuation.

379 In contrast, at sites showing ClO_4^- concentrations < 10 µg·L^{-1} (FA, FBN1, FP1 and FPM3; Figure 6),
380 the temporal variation of ClO_4^- was significantly correlated to the groundwater level fluctuation (Table
381 5). The correlation relationship was stronger at FA and FBN1 (Adj. R^2 = 0.42 and 0.54, respectively;
382 Table 5) with larger groundwater level fluctuation; at FP1 and FPM3 where the groundwater level
383 fluctuated less, the correlation relationship was weaker (Adj. R^2 = 0.35 and 0.20, respectively; Table
384 5). Diffuse sources of ClO_4^- were presumed to be present at these sites. During low water level periods,
385 most of the sources were apparently disconnected from the saturated zone. As water level rose, the

contamination source was re-activated and more contaminants were released in water and flushed into the saturated zone, resulting in the increase of ClO_4^- concentrations.

Table 5 : Correlation of ClO_4^- with groundwater levels and major ion concentrations. Values correspond to Adj. R^2 issued from the generalized additive model (statistically significant as the P-value < 0.05, related Adj. R^2 values when P-value < 0.05 are marked in bold; NA: not available)

Name	Water level	Cl^-	NO_3^-	SO_4^{2-}	Na^+	K^+	Mg^{2+}	Ca^{2+}
FVDV	0,07	-0,04	**0,21**	**0,37**	0,15	**0,53**	**0,41**	0,08
FBN4	0,07	0,03	**0,32**	0,24	0,03	0,18	**0,31**	0,01
FEP1	0,08	0,00	0,08	0,05	**0,32**	-0,02	-0,03	0,03
FBN5	**0,22**	**0,71**	**0,64**	0,02	**0,28**	**0,67**	**0,41**	**0,61**
FA	**0,42**	**0,54**	**0,56**	**0,68**	0,04	0,29	**0,24**	**0,64**
FBN1	**0,54**	**0,53**	**0,67**	**0,55**	-0,02	**0,62**	0,35	-0,02
FP1	**0,35**	0,17	0,25	0,23	0,28	**0,48**	-0,05	0,05
FPM3	**0,20**	-0,03	-0,04	-0,05	-0,04	0,17	**0,46**	0,18
RS1	NA	**0,61**	**0,13**	**0,53**	**0,49**	**0,37**	-0,06	0,05
RPY	NA	**0,10**	0,06	-0,01	-0,03	-0,06	-0,06	0,13
RS2	NA	**0,51**	**0,11**	**0,36**	0,02	**0,17**	**0,53**	0,13
PDO	NA	-0,05	0,06	0,01	-0,03	**0,16**	-0,03	0,19
FPM1	NA	**0,28**	**0,51**	-0,02	**0,10**	**0,33**	0,22	0,11
PP	NA	0,29	**0,02**	-0,05	0,16	0,03	0,08	-0,06

Generally, a poor correlation was observed between ClO_4^- and major ions (Table 5). The temporal evolution of ClO_4^- was compared with the chronicles of NO_3^- and Cl^-, the two major agriculture-derived ions in groundwater of the Champagne Chalk aquifer (Cao et al., 2020). At most sites, the temporal evolution of ClO_4^- was different from that of NO_3^- and Cl^- (Figure 6), indicating different origins of ClO_4^- *versus* NO_3^- and Cl^-. At FEP1, FPM1 and PP, despite the temporal heterogeneity of ClO_4^- levels, the concentrations of NO_3^- and Cl^- were stable over time (Figure 6). As described in Cao et al. (2020), estimated groundwater ages at these points were > 30 years in a piston flow model, which is related to the superficial formations limiting rapid transport of water and solutes (NO_3^- and Cl^-) from surface (agriculture-derived ions are distributed mainly in the soil area) to the saturated zone. Consequently, the aquifer receives recharge mainly from upstream of the superficial formation covered area. Water traveled laterally in the saturated zone during > 30 years and solute concentrations were greatly buffered, resulting in stable NO_3^- and Cl^- levels independent of water level fluctuation (Cao et al., 2020). The large variation of ClO_4^- concentrations, in contrast to the temporal stability of NO_3^- and Cl^-, could be interpreted as an indication that the location of ClO_4^- sources is much deeper than those of agriculture-derived ions. As groundwater levels rose, the contamination front of ClO_4^-

406 was reached, generating changes in ClO_4^- levels, despite the fact that flushing from the soil was largely
407 limited by superficial formations. At FPM3 (downstream from the borehole FPM1; Figure 2), a time
408 lag was observed between groundwater levels and concentrations of NO_3^- and Cl^-, likely as a result of
409 slow transport through the discontinuous graveluche formations. However, ClO_4^- levels varied with
410 groundwater levels without time lag, implying again that deeper ClO_4^- sources were more quickly
411 activated by the rise in water table.

412 At FA, unlike the positively correlated relationship between ClO_4^- and groundwater level, NO_3^- and Cl^-
413 were negatively correlated with groundwater level (Figure 6 and Table 5), indicating a dilution effect.
414 At this site, groundwater dating showed 75-80% of modern water by the binary mixing model,
415 indicating a water table constituted mainly by freshly percolated rainwater that favors the process of
416 dilution (Cao et al., 2020). During the rapid flow process following precipitation, the low mineralized
417 rainwater entered the aquifer resulting in decrease of NO_3^- and Cl^- concentrations. For ClO_4^-, it seemed
418 that the inputs by the potential sources of ClO_4^- in the UZ following the rise of groundwater level was
419 more important than the dilution process, which led to an increase in ClO_4^- with the groundwater level.

420 At FBN1 and FBN5, the temporal variabilities of ClO_4^-, NO_3^- and Cl^- were well correlated (Figure 6
421 and Table 5). Indeed, located near the groundwater divide line (Figure 2), deep water table levels were
422 observed (> 22 m, Table 1) and low permeability was suggested at these two sites (Cao et al., 2020).
423 According to groundwater dating, the groundwater flow was well described by the exponential mixing
424 model (mean residence time of < 20 years), indicating a spatially uniform recharge (Cao et al., 2020).
425 ClO_4^-, NO_3^- and Cl^- were thus flushed from the potential sources located in the UZ following recharge,
426 showing a similar temporal variation.

427 At RPY (Py River) and RS2 (Suippe River after the confluence of Py River), a decrease in ClO_4^-
428 concentration was observed during high flow period (May 2018 and May 2019; Figure 6), implying a
429 dilution effect on ClO_4^- concentration. Indeed, the rivers are recharged by the Chalk aquifer with little
430 surface runoff produced. In river valleys, the Chalk is usually highly fractured with shallow
431 groundwater levels and preferential flow of rainwater is favored especially at high water level,

resulting in dilution of the aquifer and the river water. A similar tendency was observed at PDO (pumping station near RPY), which is consistent with a mixture of groundwater and surface water as implied by groundwater dating (30% to 60% of modern water and an end-member of ~40-year old water; Cao et al., 2020).

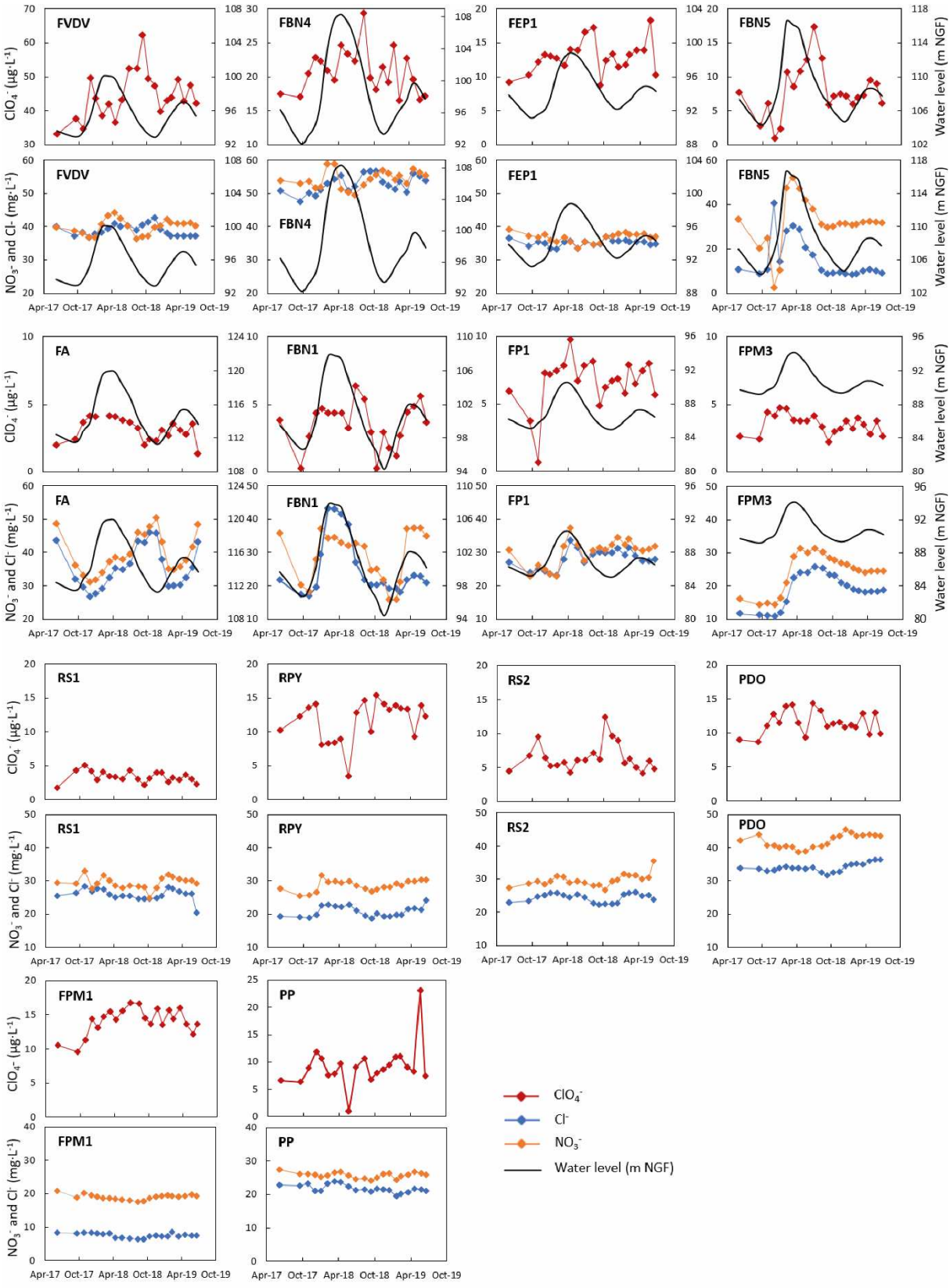

Figure 6 : Temporal variation of perchlorate concentrations compared with groundwater level fluctuations from June 2017 to June 2019

439 The potential sources of ClO_4^- located deeper than the sources of agriculture-derived ions in the UZ
440 refer most probably to unexploded ordnance still present underground after WWI. Indeed, some shells
441 fired during the war could reach > 10 meters underground without exploding (UNMAS, 2015).
442 Unused ammunitions could still be present underground in military tunnels of WWI. In addition, in the
443 Champagne Mounts area, some unused ammunitions could have been cleaned up by burying in
444 specified boreholes (Debant, 2019). Over time, the release of the explosive charge occurs as a result of
445 the general corrosion of the envelope and/or its perforation. The time required for perforation was
446 estimated between 250 and 450 years, at a rate of 1 mm/year on average (Parker et al., 2004). These
447 unexploded ordnances can be difficult to locate and clean up due to their number and their deep
448 underground location. Contamination plumes observed at some sites indicate that the ammunition
449 destruction sites may be the main point sources of ClO_4^-, as repeated detonation causes an
450 accumulation of residual ClO_4^- at these sites. The residue of ammunition destroyed by detonation can
451 persist for more than 100 years in soils (Hubé, 2014). Despite the huge quantities of fully exploded
452 ordnance, their residue is estimated at around 0.01% and can only persist for a short time underground,
453 representing a relatively small contribution to the ClO_4^- contamination of groundwater. Considering
454 that most of the potential sources of ClO_4^- have long persistence times, the ClO_4^- contamination in
455 groundwater of the study area may not decline in the short to medium term.

456 ### 3.3 Mass flow rate of perchlorate

457 In the Suippe River and its tributaries (Figure 4), the mass flow rate of ClO_4^- (M) has been estimated
458 according to the measured water flow rate (Q) and ClO_4^- concentrations (C):

459 $$M = C \times Q \quad (1)$$

460 The data of water flow rate and ClO_4^- concentration used for calculation was measured on October
461 2017. The estimated mass flow rate of ClO_4^- was 4.6 kg·month^{-1} upstream the Suippe River (RS1) and
462 13.5 kg·month^{-1} downstream of its confluence with the Py River (RS2) (Table 2). The increase of mass
463 flow rate from RS1 to RS2 (8.9 kg·month^{-1}) was approximately equal to the contribution from Py

River (9.6 kg·month^{-1}), implying that the contribution from the Chalk aquifer between RS1 and RS2 is negligible with low groundwater discharge and low ClO_4^- concentrations in the riparian aquifer.

The estimated mass flow rate of ClO_4^- downstream along the Suippe River (RS3) was 14.6 kg·month^{-1}. The Arnes River, which joins the Suippe River between RS2 and RS3, has a ClO_4^- flux less than 0.1 kg·month^{-1}. The increase of ClO_4^- mass flow rate from RS2 to RS3 (1.1 kg·month^{-1}) was due to the contribution of Chalk aquifer discharge (zero runoff is assumed on the Champagne Chalk). The groundwater discharge from RS2 to RS3 was 322 L·s^{-1}, estimated from the water flow rate at RS2, RS3 and RA. According to equation (1), a ClO_4^- concentration of 1.3 µg·L^{-1} in aquifer discharge on October 2017 was estimated, which represents the average concentration from the Chalk aquifer of left and right bank of the Suippe River.

Table 2 : Mass flow rate of ClO_4^- in the Suippe River and its tributaries (data measured on October 2017)

Name	Location	Water flow rate (L·s^{-1})	ClO_4^- concentration (µg·L^{-1})	ClO_4^- mass flow rate (kg·month^{-1})
RS1	Suippe River	401	4.3	4.6
RS2	Suippe River	752	6.7	13.5
RS3	Suippe River	1184	4.6	14.6
RPY	Py River	276	12.3	9.1
RA	Arnes River	110	< 0.5	< 0.1

The estimated monthly ClO_4^- flow rate on October 2017 represents approximately the minimum level in the Suippe River and its tributaries, as the water flow rate was measured during low discharge period, whereas ClO_4^- concentrations in rivers were relatively stable over time according to the low values of standard deviations presented in Table 1.

4 Conclusions and perspectives

This study examined sources and evolution of ClO_4^- contamination in groundwater of NE France. The NE region of France is suspected to have multiple sources of ClO_4^- related to military activities of WWI and/or the past use of Chilean nitrate as fertilizer in agriculture. An intensive sampling network was established on a study area of a representative watershed, where ClO_4^- concentrations were monitored monthly for two years (2017-2019). The measured concentrations and isotopic contents of ClO_4^- and the historical investigations have been combined with previously published data on

groundwater dating as well as hydrologic and geochemical characteristics of the Chalk aquifer (Cao et al. 2020), which allowed to clarify the sources of ClO_4^- and to understand its evolution in groundwater.

This work produced the first precise ClO_4^- contamination mapping in the study area east of Reims city with ClO_4^- concentrations in ground- and surface water ranging from < 0.5 to 62.5 $\mu g \cdot L^{-1}$. About half of the sampling sites showed ClO_4^- concentrations > 4 $\mu g \cdot L^{-1}$ and most of these sites were located downgradient of the Champagne Mounts area, where huge quantities of ClO_4^- were used, stored, or destroyed during and after WWI. Point sources of ClO_4^- were presumed to exist in the study area, as indicated by the plume-like patterns of contamination observed at some sites. The isotopic signature of ClO_4^- at the two most contaminated sites showed a synthetic origin, proving the military source of ClO_4^- contamination in the study area. In addition, the estimated groundwater ages in the study area were < 50 years, implying that ClO_4^- contamination is related to sources that may still persist in the subsoil long after the end of WWI (e.g., unexploded ammunition) or post-WWI military activities (e.g., destruction of ammunition). The isotopic analysis of ClO_4^- in river water showed a minor but distinct component of Atacama ClO_4^-, indicating the presence of some Chilean nitrate in the watershed.

Annual variations of ClO_4^- concentration were observed, indicating the influence of recharge processes and groundwater levels on ClO_4^- contamination. Two major temporal trends of ClO_4^- concentration were observed: 1) ClO_4^- concentrations poorly correlated to groundwater level with peaks of contamination due to flushing at sites having ClO_4^- concentrations > 10 $\mu g \cdot L^{-1}$, implying the presence of point sources; 2) ClO_4^- concentrations highly correlated to groundwater level at sites showing ClO_4^- concentrations < 10 $\mu g \cdot L^{-1}$, where diffuse sources were suggested. In addition, the rapid response of ClO_4^- concentration following the rise of groundwater level compared with relatively stable concentrations of agricultural ions at some sites indicated that the location of ClO_4^- sources could be much deeper than those of agricultural ions (mainly in the soil area). Considering the long persistence time of the explosive residues related to unexploded ammunitions and ammunition destruction activities, the ClO_4^- contamination in groundwater of the study area seems unlikely to decrease in the short- to medium-term.

512 The multi-tool methodology developed in the study area could furtherly be applied to other ClO_4^-
513 contaminated sites in NE France with suspected military and agricultural sources, with the aim of
514 making appropriate recommendations for a long-term management of groundwater resources.
515 Moreover, this characterization methodology could more widely applicable elsewhere in Chalk
516 aquifers or other multi-porosity mediums for the prediction of solute transport (natural or
517 anthropogenic) and for the evaluation of aquifer vulnerability. However, this research can be improved
518 and developed in several different aspects. The continuous monitoring of ClO_4^- concentrations and
519 geochemistry can be continued to obtain longer time series, with the aim to confirm and specify our
520 conclusions and also to study the evolution of ClO_4^- in the Chalk aquifer under different climate
521 conditions. More measurements of water flow rate in rivers can be realized (during low, medium and
522 high discharge period) in order to better estimate the mass flow rate of ClO_4^-. In addition, groundwater
523 sampling and analysis should also be realized at different depths of boreholes to obtain vertical
524 profiles of ClO_4^- concentrations as well as other chemical characteristics, which allows to explore their
525 relationships and to further confirm the position of potential ClO_4^- sources underground. In this study,
526 isotopic analysis of ClO_4^- has only been realized at sites with high levels of ClO_4^-. This analysis should
527 also be performed at sites having low concentrations of ClO_4^- to further confirm whether traces of
528 Atacama ClO_4^- exist on these low contaminated sites related to diffuse sources. Finally,
529 hydrogeochemical numerical modeling tools could be a relevant complement of this study to better
530 understand the transfer mechanism of ClO_4^- in the Chalk groundwater.

531 ## Declaration of Competing Interest

532 The authors declare that they have no known competing financial interests or personal relationships
533 that could have appeared to influence the work reported in this paper.

534 ## Acknowledgements

535 This work was co-funded by the BRGM, the Agence de l'Eau Seine-Normandie, the Region Grand-Est,
536 the Grand-Reims Metropole and ARS Grand-Est. Authors want to thank Nicolas Caillon of University

of Joseph Fourier Grenoble for the NO_3^- isotopic analysis; Alexandre Conreux and Julien Hubert of Gegenaa laboratory in University of Reims Champagne-Ardenne for their contribution in sampling campaigns and major ions analysis; and Alain Devos, Alexis Carlu, Thibaud Damien and Sarah Bambara for their participation in river flow measurement. Authors would also like to thank the owners and operators for access to their boreholes.

References

Allen, D.J., Brewerton, L.J., Coleby, L.M., Gibbs, B.R., Lewis, M.A., MacDonald, A.M., Wagstaff, S.J., Williams, A.T., 1997. The physical properties of major aquifers in England and Wales. British Geological Survey Technical Report WD/97/34, 312 p.

Allouc, J., Le Roux, J., Batkowski, D., Bourdillon, C., Catillon, J., Causero, L., Ménillet, F., Morfaux, P., Ravaux, P., 2000. Notice explicative, Carte géol. France (1/50 000), feuille Suippes (159).Orléans: BRGM, 73 p. Carte géologique par Allouc, J. et Le Roux, J. (2000)

ANSES, 2018. Avis de l'Anses relatif à la « Pertinence de la ré-évaluation de la valeur guide pour les ions perchlorate dans l'eau destinée à la consommation humaine ». Maison-Alfort, Anses, 42 p.

ANSES, 2013. Campagne nationale d'occurrence de polluants émergents dans les eaux destinées à la consommation humaine. Maison-Alfort, Anses, 56 p.

ANSES, 2011. Avis de l'Anses relatif à l'évaluation des risques sanitaires liés à la présence d'ions perchlorate dans les eaux destinées à la consommation humaine. Maison-Alfort, Anses, 22 p.

Aziz, C., Borch, R., Nicholson, P., Cox, E., 2006. Alternative Causes of Wide-Spread, Low Concentration Perchlorate Impacts to Groundwater, in: Perchlorate: Environmental Occurrence, Interactions and Treatment. Springer, Boston, MA, pp. 71–91. https://doi.org/10.1007/0-387-31113-0_4

Bao, H., Gu, B., 2004. Natural perchlorate has a unique oxygen isotope signature. Environ. Sci. Technol. 38, 5073–5077.

Barhoum, S., Valdès, D., Guérin, R., Marlin, C., Vitale, Q., Benmamar, J., Gombert, P., 2014. Spatial heterogeneity of high-resolution Chalk groundwater geochemistry – Underground quarry at Saint Martin-le-Noeud, France. Journal of Hydrology 519, 756–768. https://doi.org/10.1016/j.jhydrol.2014.08.001

Barraclough, D., Gardner, C.M.K., Wellings, S.R., Cooper, J.D., 1994. A tracer investigation into the importance of fissure flow in the unsaturated zone of the British Upper Chalk. Journal of Hydrology 156, 459–469. https://doi.org/10.1016/0022-1694(94)90090-6

BASOL database. https://basol.developpement-durable.gouv.fr/. Accessed date: October 2019.

Bausinger, T., Bonnaire, E., Preuß, J., 2007. Exposure assessment of a burning ground for chemical ammunition on the Great War battlefields of Verdun. Science of The Total Environment 382, 259–271. https://doi.org/10.1016/j.scitotenv.2007.04.029

Böhlke, J.K., Ericksen, G.E., Revesz, K., 1997. Stable isotope evidence for an atmospheric origin of desert nitrate deposits in northern Chile and southern California, U.S.A. Chem. Geol. 136, 135152. https://doi.org/10.1016/S0009-2541(96)00124-6

Böhlke, J.K., Hatzinger, P.B., Sturchio, N.C., Gu, B., Abbene, I., Mroczkowski, S.J., 2009. Atacama perchlorate as an agricultural contaminant in groundwater: isotopic and chronologic evidence from Long Island, New York. Environ. Sci. Technol. 43, 5619–5625.

Böhlke, J.K., Mroczkowski, S.J., Sturchio, N.C., Heraty, L.J., Richman, K.W., Sullivan, D.B., Griffith, K.N., Gu, B., Hatzinger, P.B., 2017. Stable isotope analyses of oxygen (18O:17O:16O) and chlorine (37Cl:35Cl) in perchlorate: reference materials, calibrations, methods, and interferences. Rapid Commun. Mass Spectrom. 31, 85–110. https://doi.org/10.1002/rcm.7751

Böhlke, J.K., Sturchio, N.C., Gu, B., Horita, J., Brown, G.M., Jackson, W.A., Batista, J., Hatzinger, P.B., 2005. Perchlorate Isotope Forensics. Anal. Chem. 77, 7838–7842. https://doi.org/10.1021/ac051360d

Brabant, G., Bergmann, P., Kirsch, C.M., Köhrle, J., Hesch, R.D., von zur Mühlen, A., 1992. Early adaptation of thyrotropin and thyroglobulin secretion to experimentally decreased iodine supply in man. Metabolism 41, 1093–1096. https://doi.org/10.1016/0026-0495(92)90291-H

Braverman, L.E., He, X., Pino, S., Cross, M., Magnani, B., Lamm, S.H., Kruse, M.B., Engel, A., Crump, K.S., Gibbs, J.P., 2005. The effect of perchlorate, thiocyanate, and nitrate on thyroid function in workers exposed to perchlorate long-term. J. Clin. Endocrinol. Metab. 90, 700–706. https://doi.org/10.1210/jc.2004-1821

Brouyère, S., Dassargues, A., Hallet, V., 2004. Migration of contaminants through the unsaturated zone overlying the Hesbaye chalky aquifer in Belgium: a field investigation. Journal of Contaminant Hydrology 72, 135–164. https://doi.org/10.1016/j.jconhyd.2003.10.009

Brown, G.M., Gu, B., 2006. The Chemistry of Perchlorate in the Environment, in: Perchlorate: Environmental Occurence, Interactions and Treatment. Springer, Boston, MA, pp. 17–47. https://doi.org/10.1007/0-387-31113-0_2

Cao, F., Jaunat, J., Ollivier, P., Cancès, B., Morvan, X., Hubé, D., Devos, A., Devau, N., Barbin, V., Pannet, P., 2018. Sources and behavior of perchlorate ions (ClO_4^-) in chalk aquifer of Champagne-Ardenne, France: preliminary results, in: IAHS-AISH Proceedings and Reports, 8th International Water Resources Management Conference of ICWRS, June 2018, Beijing (China). pp. 113–117. https://doi.org/10.5194/piahs-379-113-2018

Cao, F., Jaunat, J., Sturchio, N., Cancès, B., Morvan, X., Devos, A., Barbin, V., Ollivier, P., 2019. Worldwide occurrence and origin of perchlorate ion in waters: A review. Sci. Total Environ. 661, 737–749. https://doi.org/10.1016/j.scitotenv.2019.01.107

Cao, F., Jaunat, J., Vergnaud-Ayraud, V., Devau, N., Labasque, T., Guillou, A., Guillaneuf, A., Hubert, J., Aquilina, L., Ollivier, P., 2020. Heterogeneous behavior of unconfined Chalk aquifers infer from combination of groundwater residence time, hydrochemistry and hydrodynamic tools. Journal of Hydrology 581, 124433. https://doi.org/10.1016/j.jhydrol.2019.124433

Chen, N., Valdes, D., Marlin, C., Blanchoud, H., Guerin, R., Rouelle, M., Ribstein, P., 2019. Water, nitrate and atrazine transfer through the unsaturated zone of the Chalk aquifer in northern France. Science of The Total Environment 652, 927–938. https://doi.org/10.1016/j.scitotenv.2018.10.286

Chiesi, F., 1993. Transfert et epuration dans la zone non saturee de la craie en champagne : etude de quelques cas concernant les nitrates et l'atrazine. PhD thesis, Reims, 197 p.

Clausen, J.L., Korte, N., Dodson, M., Robb, J., Rieven, S., 2006. Conceptual Model for the Transport of Energetic Residues from Surface Soil to Groundwater by Range Activities. Cold regions research and engineering lab, Final report, ERDC/CRREL-TR-06-18, 169 p.

CORINE land cover database. https://www.geoportail.gouv.fr/donnees/corine-land-cover-2018. Accessed date: October 2019.

621 Crampon, N., J. C. Roux, Bracq, P., 1993, Hydrogeology of the chalk in France, in The Hydrogeology
622 of the Chalk of North-West Europe, edited by R. A. Downing, M. Price, and G. P. Jones,
623 Oxford Univ. Press, New York, pp. 81–123.

624 Debant, J., 2019. La lente dépollution du CEA de Moronvilliers. L'hebdo du vendredi.
625 http://www.lhebdoduvendredi.com/article/36274/la-lente-depollution-du-cea-de-moronvilliers.
626 Accessed date : December 5, 2019.

627 Desailloud, R., Wemeau, J.-L., 2016. Faut-il craindre les ions perchlorate dans l'environnement ? La
628 Presse Médicale, Médecine et environnement 45, 107–116.
629 https://doi.org/10.1016/j.lpm.2015.10.002

630 Edmunds, W.M., Cook, J.M., Darling, W.G., Kinniburgh, D.G., Miles, D.L., Bath, A.H., Morgan-
631 Jones, M., Andrews, J.N., 1987. Baseline geochemical conditions in the Chalk aquifer,
632 Berkshire, U.K.: a basis for groundwater quality management. Applied Geochemistry 2, 251–
633 274. https://doi.org/10.1016/0883-2927(87)90042-4

634 Ericksen, G.E., 1983. The Chilean nitrate deposits. Am. Sci. 71, 366–374.

635 Facon, P., 2018. Les batailles des monts de Champagne 1914-1918. Editions Tranchées, Paris :
636 Louviers, 239 p.

637 Foster, S.S.D., 1975. The Chalk groundwater tritium anomaly — A possible explanation. J. Hydrol. 25,
638 159–165. https://doi.org/10.1016/0022-1694(75)90045-1

639 Furdui, V.I., Zheng, J., Furdui, A., 2018. Anthropogenic Perchlorate Increases since 1980 in the
640 Canadian High Arctic. Environ. Sci. Technol. 52, 972–981.
641 https://doi.org/10.1021/acs.est.7b03132

642 Greer, M.A., Goodman, G., Pleus, R.C., Greer, S.E., 2002. Health effects assessment for
643 environmental perchlorate contamination: the dose response for inhibition of thyroidal
644 radioiodine uptake in humans. Environ. Health Perspect. 110, 927–937.

645 Gu, B., Böhlke, J.K., Sturchio, N.C., Hatzinger, P.B., Jackson, W.A., Beloso Jr., A.D., Heraty, L.J.,
646 Bian, Y., Jiang, X., Brown, G.M., 2011. Removal, Recovery and Fingerprinting of Perchlorate
647 by Ion Exchange Processes in Ion Exchange And Solvent Extraction: a Series of Advances,
648 twentieth ed. Taylor and Francis Group, New York, pp. 117–144.

649 Gu, B., Brown, G.M., 2006. Recent Advances in Ion Exchange for Perchlorate Treatment, Recovery
650 and Destruction, in: Gu, B., Coates, J.D. (Eds.), Perchlorate: Environmental Occurrence,
651 Interactions and Treatment. Springer US, Boston, MA, pp. 209–251.
652 https://doi.org/10.1007/0-387-31113-0_10

653 Gu, B., Brown, G.M., Chiang, C.-C., 2007. Treatment of Perchlorate-Contaminated Groundwater
654 Using Highly Selective, Regenerable Ion-Exchange Technologies. Environ. Sci. Technol. 41,
655 6277–6282. https://doi.org/10.1021/es0706910

656 Gu, B., Brown, G.M., Maya, L., Lance, M.J., Moyer, B.A., 2001. Regeneration of Perchlorate (ClO4-
657)-Loaded Anion Exchange Resins by a Novel Tetrachloroferrate (FeCl4-) Displacement
658 Technique. Environ. Sci. Technol. 35, 3363–3368. https://doi.org/10.1021/es010604i

659 Hatzinger, P.B., Böhlke, J.K., Sturchio, N.C., Izbicki, J., Teague, N., 2018. Four-dimensional isotopic
660 approach to identify perchlorate sources in groundwater: Application to the Rialto-Colton and
661 Chino subbasins, southern California (USA). Applied Geochemistry 97, 213–225.
662 https://doi.org/10.1016/j.apgeochem.2018.08.020

663 Hatzinger, P.B., Böhlke, J.K., Sturchio, N.C., Gu, B., 2011. Guidance Document: Validation of
664 chlorine and oxygen isotope ratio analysis to differentiate perchlorate sources and to document
665 perchlorate biodegradation U.S. Department of Defense, ESTCP Project ER-200509, 107 p.
666 (available at https://www.serdp-estcp.org/Program-Areas/Environmental-

667 Restoration/Contaminated-Groundwater/Emerging-Issues/ER-200509/ER-
668 200509/(language)/eng-US

669 Headworth, H.G., Keating, T., Packman, M.J., 1982. Evidence for a shallow highly-permeable zone in
670 the Chalk of Hampshire, U.K. J. Hydrol. 55, 93–112. https://doi.org/10.1016/0022-
671 1694(82)90122-6

672 Hubé, D., 2016. Sur les traces d'un secret enfoui: Enquête sur l'héritage toxique de la Grande Guerre -
673 Préface de Jean-Yves Le Naour. Editions Michalon. 288 p.

674 Hubé, D., 2014. Perchlorates : éléments historiques et d'expertise pour une évaluation de l'impact
675 environnemental. http://centenaire.org/fr/espace-scientifique/societe/perchlorates-elements-
676 historiques-et-dexpertise-pour-une-evaluation-de (Accessed date: 15 October 2019).

677 Hubé, D., Bausinger, T., 2013. Marquage pyrotechnique : analyse de la problématique
678 environnementale. Comparatif entre Allemagne et France. Géologues 32–38.

679 IGN Remonter le temps database. https://remonterletemps.ign.fr/. Accessed October 2019.

680 Jackson, W.A., Böhlke, J.K., Andraski, B.J., Fahlquist, L., Bexfield, L., Eckardt, F.D., Gates, J.B.,
681 Davila, A.F., McKay, C.P., Rao, B., Sevanthi, R., Rajagopalan, S., Estrada, N., Sturchio, N.,
682 Hatzinger, P.B., Anderson, T.A., Orris, G., Betancourt, J., Stonestrom, D., Latorre, C., Li, Y.,
683 Harvey, G.J., 2015. Global patterns and environmental controls of perchlorate and nitrate co-
684 occurrence in arid and semi-arid environments. Geochim. Cosmochim. Acta 164, 502–522.
685 https://doi.org/10.1016/j.gca.2015.05.016

686 Jackson, W.A., Böhlke, J.K., Gu, B., Hatzinger, P.B., Sturchio, N.C., 2010. Isotopic composition and
687 origin of indigenous natural perchlorate and co-occurring nitrate in the southwestern United
688 States. Environ. Sci. Technol. 44, 4869–4876. https://doi.org/10.1021/es903802j

689 Jackson, A., Davila, A.F., Böhlke, J.K., Sturchio, N.C., Sevanthi, R., Estrada, N., Brundrett, M.,
690 Lacelle, D., McKay, C.P., Poghosyan, A., Pollard, W., Zacny, K., 2016. Deposition,
691 accumulation, and alteration of Cl^-, NO_3^-, ClO_4^- and ClO_3^- salts in a hyper-arid polar
692 environment: Mass balance and isotopic constraints. Geochimica et Cosmochimica Acta 182,
693 197–215. https://doi.org/10.1016/j.gca.2016.03.012

694 Jackson, W.A., Kumar Anandam, S., Anderson, T., Lehman, T., Rainwater, K., Rajagopalan, S.,
695 Ridley, M., Tock, R., 2005. Perchlorate occurrence in the Texas Southern High Plains Aquifer
696 System. Ground Water Monit. Remediat. 25, 137–149. https://doi.org/10.1111/j.1745-
697 6592.2005.0009.x

698 Jaunat, J., Taborelli, P., Devos, A., 2018. Les impacts de La Grande Guerre sur la qualité des eaux
699 souterraines: les cas des perchlorate, in: « 14-18 La Terre et Le Feu Géologie et Géologues
700 Sur Le Front Occidental », Bergerat, F. (Dir.), Co-Éd. AGBP – COFRHIGEO – SGN, Mém.
701 Hors-Série N°10 de l'AGBP, 414- 417.

702 Kannan, K., Praamsma, M.L., Oldi, J.F., Kunisue, T., Sinha, R.K., 2009. Occurrence of perchlorate in
703 drinking water, groundwater, surface water and human saliva from India. Chemosphere 76,
704 22–26. https://doi.org/10.1016/j.chemosphere.2009.02.054

705 Laurain, M., Guérin, H., Durand, R., Chertier, B., Louis, P., Morfaux, P., Neiss, R., 1981. Notice
706 explicative, Carte géol. France (1/50 000) feuile Reims (132). Orléans : BRGM, 34 p. Carte
707 géol. France par Laurain, M., Guérin, H., Barta, L., Monciardini, Ch., Durand, R., Neiss, R.,
708 1981.

709 Laurent, A., 1988. La Grande Guerre en Champagne et la deuxième victoire de la Marne. Secrétariat
710 d'État aux anciens combattants, Le Coteau, 157 p.

711 Lopez, B., Brugeron, A., Devau, N., Ollivier, P., 2014. Vulnérabilité des eaux souterraines de France
712 métropolitaine vis-à-vis des ions perchlorates. Rapport BRGM/RP-63270-FR, 108 p.

Lopez, B., Vernoux, J.F., Neveux, A., Barrez, F., Brugeron, A., 2015. Recherche des origines de la pollution en perchlorate impactant des captages au sein des AAC de la région de Nemours et Bourron-Marlotte. Rapport BRGM/RP-64840-FR, 140 p.

Lybrand, R.A., Bockheim, J.G., Ge, W., Graham, R.C., Hlohowskyj, S.R., Michalski, G., Prellwitz, J.S., Rech, J.A., Wang, F., Parker, D.R., 2016. Nitrate, perchlorate, and iodate co-occur in coastal and inland deserts on Earth. Chem. Geol. 442, 174–186. https://doi.org/10.1016/j.chemgeo.2016.05.023

Mangeret, A., De Windt, L., Crançon, P., 2012. Reactive transport modelling of groundwater chemistry in a chalk aquifer at the watershed scale. J. Contam. Hydrol. 138–139, 60–74. https://doi.org/10.1016/j.jconhyd.2012.06.004

Mathias, S.A., Butler, A.P., Jackson, B.M., Wheater, H.S., 2006. Transient simulations of flow and transport in the Chalk unsaturated zone. Journal of Hydrology, Hydro-ecological functioning of the Pang and Lambourn catchments, UK 330, 10–28. https://doi.org/10.1016/j.jhydrol.2006.04.010

McLaughlin, C.L., Blake, S., Hall, T., Harman, M., Kanda, R., Hunt, J., Rumsby, P.C., 2011. Perchlorate in raw and drinking water sources in England and Wales. Water Environ. J. 25, 456–465. https://doi.org/10.1111/j.1747-6593.2010.00237.x

Michalski, G., Kolanowski, M., Riha, K.M., 2015. Oxygen and nitrogen isotopic composition of nitrate in commercial fertilizers, nitric acid, and reagent salts. Isotopes Environ. Health Stud. 51, 382–391. https://doi.org/10.1080/10256016.2015.1054821

Morin, S., Savarino, J., Frey, M.M., Domine, F., Jacobi, H.-W., Kaleschke, L., Martins, J.M.F., 2009. Comprehensive isotopic composition of atmospheric nitrate in the Atlantic Ocean boundary layer from 65°S to 79°N. J. Geophys. Res. Atmospheres 114. https://doi.org/10.1029/2008JD010696

Parker, B., Chendorain, M., Stewart, L., 2004. UXO Corrosion - Potential Contamination Source. SERDP Project ER-1226, 95 p.

Poghosyan, A., Sturchio, N.C., Morrison, C.G., Beloso, A.D., Guan, Y., Eiler, J.M., Jackson, W.A., Hatzinger, P.B., 2014. Perchlorate in the Great Lakes: isotopic composition and origin. Environ. Sci. Technol. 48, 11146–11153. https://doi.org/10.1021/es502796d

Price, M., 1987. Fluid flow in the Chalk of England. Geol. Soc. Lond. Spec. Publ. 34, 141–156. https://doi.org/10.1144/GSL.SP.1987.034.01.10

Qin, X., Zhang, T., Gan, Z., Sun, H., 2014. Spatial distribution of perchlorate, iodide and thiocyanate in the aquatic environment of Tianjin, China: environmental source analysis. Chemosphere 111, 201–208. https://doi.org/10.1016/j.chemosphere.2014.03.082

Quinn, M.J., 2015. Chapter 11 - Wildlife Toxicity Assessment for Nitrocellulose, in: Williams, M.A., Reddy, G., Quinn, M.J., Johnson, M.S. (Eds.), Wildlife Toxicity Assessments for Chemicals of Military Concern. Elsevier, pp. 217–226. https://doi.org/10.1016/B978-0-12-800020-5.00011-9

Rajagopalan, S., Anderson, T.A., Fahlquist, L., Rainwater, K.A., Ridley, M., Jackson, W.A., 2006. Widespread presence of naturally occurring perchlorate in high plains of Texas and New Mexico. Environ. Sci. Technol. 40, 3156–3162.

Rao, B., Anderson, T.A., Orris, G.J., Rainwater, K.A., Rajagopalan, S., Sandvig, R.M., Scanlon, B.R., Stonestrom, D.A., Walvoord, M.A., Jackson, W.A., 2007. Widespread natural perchlorate in unsaturated zones of the southwest United States. Environ. Sci. Technol. 41, 4522–4528.

R Core Team, 2018. R: A Language and Environment for Statistical Computing. R Foundation for Statistical Computing, Vienna. https://www.R-project.org

Ricour, J., 2013. Un exemple d'altération du fond géochimique naturel des sols et des eaux souterraines : les séquelles environnementales des grands conflits mondiaux en France. Géologues 179, 27–31.

Rouxel-David, E., Batkowski, D., Baudouin, V., Cordonnier, G., Cubizolles, J., Herrouin, J.P., Izac, J.L., Jegou, J.P., Kieffer, C., Mardhel, V., Paya, H., 2002. Cartographie de la piézométrie de la nappe de la craie en Champagne-Ardenne, Rapport BRGM/RP-52332-FR, 29 p.

Savarino, J., Morin, S., Erbland, J., Grannec, F., Patey, M.D., Vicars, W., Alexander, B., Achterberg, E.P., 2013. Isotopic composition of atmospheric nitrate in a tropical marine boundary layer. Proc. Natl. Acad. Sci. 110, 17668–17673. https://doi.org/10.1073/pnas.1216639110

Serrano-Nascimento, C., Calil-Silveira, J., Dalbosco, R., Zorn, T.T., Nunes, M.T., 2018. Evaluation of hypothalamus-pituitary-thyroid axis function by chronic perchlorate exposure in male rats. Environ. Toxicol. 33, 209–219. https://doi.org/10.1002/tox.22509

Sturchio, N.C., Beloso, A., Heraty, L.J., Wheatcraft, S., Schumer, R., 2014. Isotopic tracing of perchlorate sources in groundwater from Pomona, California. Appl. Geochem. 43, 80–87. https://doi.org/10.1016/j.apgeochem.2014.01.012

Sturchio, N.C., Böhlke, J.K., Gu, B., Hatzinger, P.B., Jackson, W.A., 2011. Isotopic Tracing of Perchlorate in the Environment, in: Handbook of Environmental Isotope Geochemistry, Advances in Isotope Geochemistry. Springer, Berlin, Heidelberg, pp. 437–452. https://doi.org/10.1007/978-3-642-10637-8_22

Sturchio, N.C., Böhlke, J.K., Gu, B., Horita, J., Brown, G.M., Beloso Jr., A.D., Patterson, L.J., Hatzinger, P.B., Jackson, W.A., Batista, J., 2006. Stable isotopic composition of chlorine and oxygen in synthetic and natural perchlorate, in: Perchlorate: Environmental Occurrence, Interactions and Treatment. pp. 93–109. https://doi.org/10.1007/0-387-31113-0_5

Sturchio, N.C., Caffee, M., Beloso, A.D., Heraty, L.J., Böhlke, J.K., Hatzinger, P.B., Jackson, W.A., Gu, B., Heikoop, J.M., Dale, M., 2009. Chlorine-36 as a tracer of perchlorate origin. Environ. Sci. Technol. 43, 6934–6938.

Taborelli, P., 2018. Les conditions géographiques et l'organisation spatiale du front de la Grande Guerre : application à l'évaluation environnementale post-conflit en Champagne-Ardenne (France) Phd thesis, Reims, 427 p.

Trumpolt, C.W., Crain, M., Cullison, G.D., Flanagan, S.J.P., Siegel, L., Lathrop, S., 2005. Perchlorate: Sources, Uses, and Occurrences in the Environment. Remediat. J. 16, 65–89. https://doi.org/10.1002/rem.20071

Urbansky, E.T., 2002. Perchlorate as an environmental contaminant. Environ. Sci. Pollut. Res. 9, 187–192. https://doi.org/10.1007/BF02987487

Urbansky, E.T., 1998. Perchlorate Chemistry: Implications for Analysis and Remediation. Bioremediation J. 2, 81–95. https://doi.org/10.1080/10889869891214231

UNMAS, 2015. Mines terrestres, restes explosifs de guerre et engins explosifs improvisés - Manuel de sécurité, 3e édition. UNMAS - United Nations Mine Action Service, New York. 130 p.

Vachier, P., Cambier, P., Prost, J.C., 1987. Mouvements de l'eau dans la zone non sature´e et alimentation de la nappe de la craie de champagne (France). Isot. Tech. Water Resour. Dev. Vienna IAEA Conf. 367–379.

Vega, M., Nerenberg, R., Vargas, I., 2018. Perchlorate contamination in Chile: Legacy, challenges, and potential solutions. Environ. Res. 164, 316–326. https://doi.org/10.1016/j.envres.2018.02.034

Vergnaud-Ayraud, V., Aquilina, L., Pauwels, H., Labasque, T., 2008. La datation des eaux souterraines par analyse des CFC : un outil de gestion durable de la ressource en eau. Tech. Sci. Méthodes 37–44. https://doi.org/10.1051/tsm/200801037

Vernhet, Y., 2007. Carte geologique harmonisée du département de la Marne Rapport BRGM RP-55732-FR, 112 p.

Wellings, S.R., 1984. Recharge of the Upper Chalk aquifer at a site in Hampshire, England: 2. Solute movement. Journal of Hydrology 69, 275–285. https://doi.org/10.1016/0022-1694(84)90167-7

Zimmermann, M., 1917. Le nitrate du Chili. Ann. Géographie 26, 237–238.

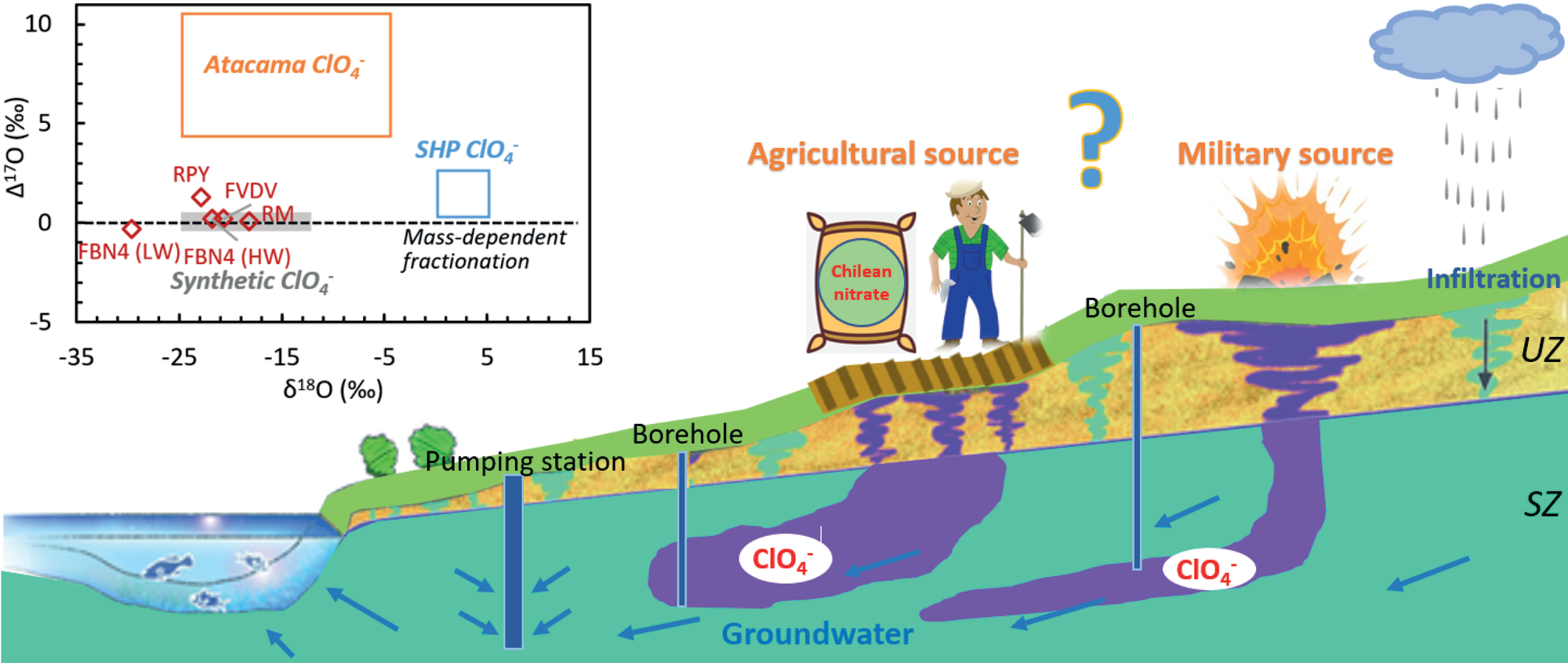
10
5
0
-5
$\Delta^{17}O$ (‰)
-35
-25
-15
-5
5
15
$\delta^{18}O$ (‰)
Atacama ClO_4^-
SHP ClO_4^-
RPY
FVDV
RM
FBN4 (LW)
FBN4 (HW)
Synthetic ClO_4^-
Mass-dependent fractionation
Agricultural source
?
Military source
Chilean nitrate
Infiltration
Borehole
UZ
Pumping station
Borehole
SZ
ClO_4^-
ClO_4^-
Groundwater